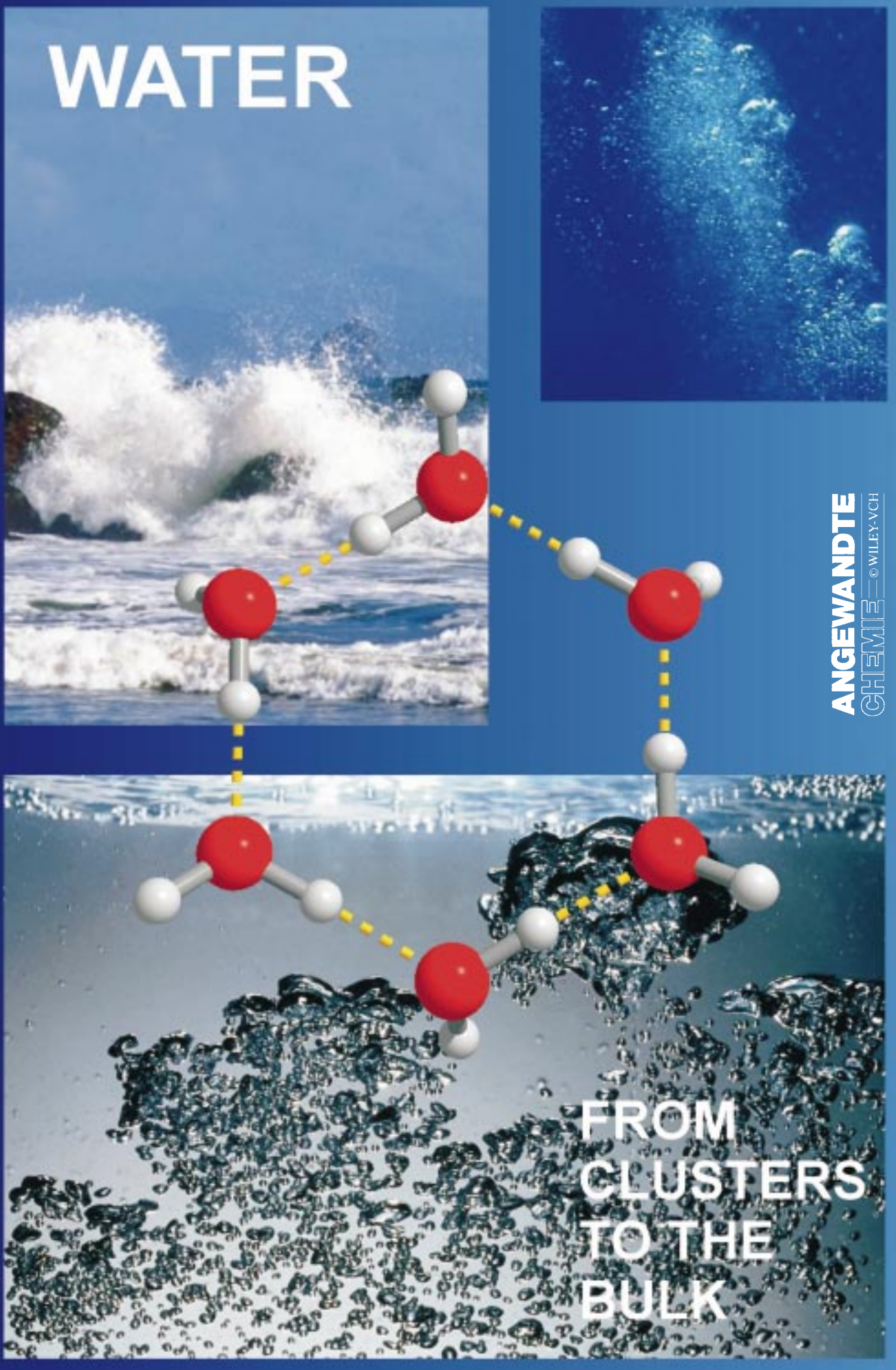

ANGEWANDTE CHEMIE © WILEY-VCH

Water: From Clusters to the Bulk

Ralf Ludwig*

Dedicated to Professor Manfred Zeidler on the occasion of his 65th birthday

Water is of fundamental importance for human life and plays an important role in many biological and chemical systems. Although water is the most abundant compound on earth, it is definitely not a simple liquid. It possesses strongly polar hydrogen bonds which are responsible for a striking set of anomalous physical and chemical properties. For more than a century the combined importance and peculiarity of water inspired scientists to construct conceptual models, which in themselves reproduce the observed behavior of the liquid. The exploration of structural and binding properties of small water complexes provides a key for understanding bulk water in its liquid and solid phase and for understanding solvation phenomena. Modern ab initio quantum chemistry methods and high-resolution spectroscopy methods have been extremely successful in describing such structures. Cluster models for liquid water try to mimic the transition from these clusters to bulk water. The important question is: What cluster properties are required to describe liquid-phase behavior?

Keywords: ab initio calculations · hydrogen bonds · molecular clusters · vibrational spectroscopy · water chemistry

1. Introduction

Water has probably received more scientific and technological interest than any other substance—mainly for two reasons. Firstly, water is a major chemical constituent of our planet's surface and as such it has been indispensable for the genesis of life. Secondly, it exhibits a fascinating array of unusual properties in pure form and as a solvent. The importance of water is clearly described in monographs such as "Properties of Ordinary Water Substance" by Dorsey (1940),[1] the compendium "Water. A Comprehensive Treatise, Volumes 1–7", edited by Franks (1972–1982),[2] the book "Metastable Liquids" by Debenedetti (1996),[3] and Ball's popular survey of the "history" of water "H_2O—A Biography of Water" (1999).[4] Those standard works go along with thousands of reviews, proceedings, and articles which all show that water is one of the most appealing of the open puzzles in science. Among those highlights, Bernal and Fowler's "A theory of water and ionic solution, with particular reference to hydrogen and hydoxyl ions",[5] Narten and Levy's "Observed diffraction pattern and proposed models of liquid water",[6] Stillinger's "Water Revisited",[7] and Mishima and Stanley's review about "The relationship between liquid, supercooled and glassy water"[8] should be emphasized.

Recent progress in some fields of water science makes it worthwhile to summarize important results obtained during the last five years. Topics concern the discovery of new ice phases,[9, 10] new insight into supercooled and glassy water,[8, 11, 12] and a better understanding of high-mobility transport of water ions.[13, 14]

In this review I would like to focus on recent progress in calculating and measuring water clusters and their properties. This interest is mainly a consequence of the fact that investigations on small water clusters are a perfect means with which to characterize structural changes and bonding mechanisms in passing from isolated molecules to bulk states. Thus we can ask whether their is a continuous path from the gas to the liquid phase. Is there some evidence from experiments or theoretical models that gas-phase structures may also be important constituents of the liquid phase?

An outline of this review is as follows: First we describe some of the anomalies of water. The fascinating array of unusual properties can be qualitatively understood from water-bonding characteristics. Thus we discuss hydrogen bonds (H-bonds) and their possible arrangements in water. The crystal structures of hexagonal ice I_h and clathrate

[*] Priv.-Doz. Dr. R. Ludwig
Physikalische Chemie
Fachbereich Chemie der Universität Dortmund
Otto-Hahn-Strasse 6, 44221 Dortmund (Germany)
Fax: (+49) 231-755-3937
E-mail: ludwig@pc2a.chemie.uni-dortmund.de

  1433-7851/01/4010-1809 $ 17.50+.50/0

hydrates are presented as typical three-dimensional networks. Many-body effects are crucial for the size and arrangement of water complexes. Consequently we discuss recent theoretical and experimental evidence for cooperativity in H-bonded systems. This chapter is followed by a brief introduction into two common water models: the mixture and the continuum model approaches.

A survey of calculated water clusters ranges from small ring structures up to icosahedral networks. The main features and properties of the water structures are discussed in respect to experimental findings and their possible relevance for water models.

In the following chapter we describe exciting spectroscopic methods which recently allowed the detection of small water clusters: small quasi-planar ring structures ($n = 3-5$), isomeric hexamers ($n = 6$) representing the transition from cyclic to three-dimensional structures, and larger clusters in the "cage" regime ($n = 7-12$). Finally we present recent cluster models for liquid water. All models are based on calculated water structures and it is assumed that these may be constituents of the liquid phase. We discuss whether these models are able to explain the properties of liquid water including some of it's anomalies.

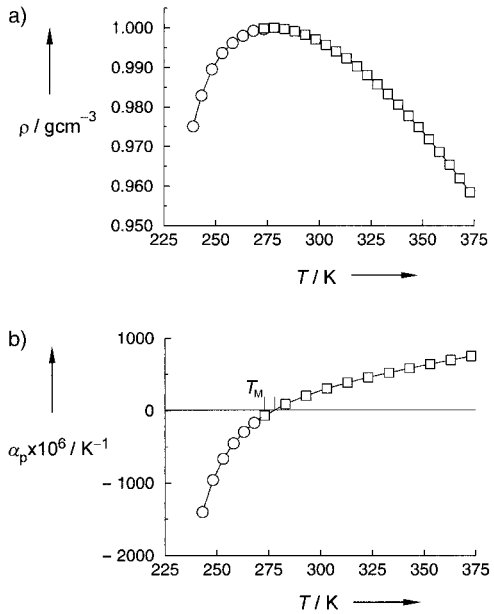

Figure 1. Temperature dependence of the isobar density ρ (a)[16, 18] and the thermal expansivity α_p (b).[19]

2. Water Anomalies

The behavior of liquid water deviates strongly from that expected of a simple liquid in almost every respect. The liquid-phase density maximum is the most prominent and publicized of the water anomalies.

The density of liquid water at atmospheric pressure increases as it is cooled to 277 K, at which temperature the density has a maximum value of 0.999972 g cm^{-3}.[15, 16] As shown in Figure 1a, the density decreases rapidly below 277 K, a trend which continues if the liquid density is followed into the supercooled region below the freezing point at 273 K.[17–19] Although water is not the only liquid to exhibit a density maximum, the phenomenon only appears in a few other liquids, such as SiO_2[20] and Ga[21] melts. Water also possesses a negative volume of melting (Figure 1b). The density of most liquids increases as they freeze, however, water expands by about 11%. It is that process that allows a sheet of ice to float on liquid water. Both effects, the density maximum and the negative volume of melting, cause lakes and rivers to freeze from the top down.

The isothermal compressibility κ_T[22] passes through a minimum in the normal liquid-water range at 319 K. It then increases further as the temperature decreases and becomes more pronounced in the supercooled region (Figure 2a). The same behavior is found for the heat capacity C_P at constant pressure.[23, 24] As shown in Figure 2b, the minimum value of C_P occurs at 308 K, which is right in the middle of the liquid-water range. Supercooling leads to a strong increase in the heat capacity. It takes more heat to raise the temperature of water than to warm up most other substances by the same amount. This occurrence results in ocean circulation effects that strongly influence local and global climates.

The dynamic properties of water also show strong deviations from simple liquid behavior. The diffusion constant D normally decreases as pressure increases at constant temper-

Ralf Ludwig, born in 1961 in Gladbeck, Germany, studied physics and graduated from the Rheinisch-Westfälische Technische Hochschule in Aachen with a diploma in 1988. Three years later he received his PhD in physical chemistry under the guidance of Prof. Manfred Zeidler. He received a research stipend from the Heinrich-Hertz-Stiftung of the state of North-Rhine-Westfalia and worked with Prof. Tom C. Farrar as a postdoctoral fellow in the chemistry department of the University of Wisconsin in Madison, where he improved his skills in liquid NMR spectroscopy. During his two-year stay in Madison he also conducted theoretical studies with Prof. Frank Weinhold. In 1995 he returned to Germany and joined the research group of Prof. Alfons Geiger at the University of Dortmund. There, he extended his methodological spectrum by molecular dynamics simulations and obtained his habilitation in physical chemistry in 1999 for studying hydrogen bonding in clusters, liquids, and oligopeptides. His current research focuses on the structure and dynamics of molecular clusters, pure liquids, and aqueous solutions of biophysical interest.

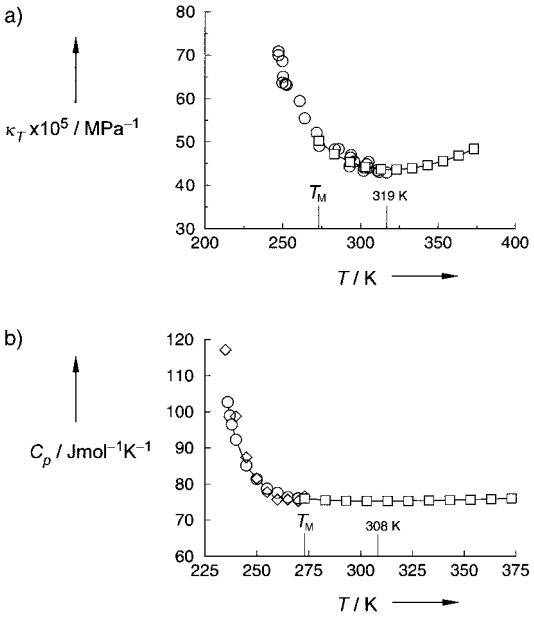

Figure 2. Temperature dependence of the isothermal compressibility k_T (a)[21] and the constant-pressure specific heat C_p (b).[22, 23]

ature. Again, liquid water displays a reversal of this behavior. As shown in Figure 3a, the diffusion coefficient actually increases with increasing pressure up to about 200 MPa, above which the usual decrease in D is observed.[25] Cold water gets more fluid when it is squeezed, whereas most

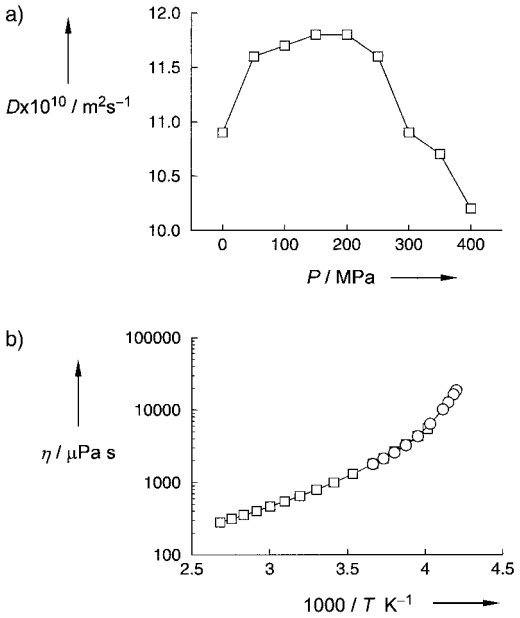

Figure 3. Pressure dependence of the isothermal diffusion coefficient D at 273 K (a)[24] and the temperature dependence of the isobaric viscosity η at atmospheric pressure (b).[25, 26]

liquids become more viscous under pressure. The pressure and temperature dependence of another transport property, the viscosity η, is also anomalous.[17, 26] Figure 3b shows an Arrhenius plot at atmospheric pressure. The deviation of the data from a straight line indicates that the activation energy E_A for the molecular motion increases with decreasing temperature, which indicates there is a change in the mechanism of molecular mobility.[27] Many other dynamic properties of the liquid, such as the dielectric relaxation time[28] and the nuclear spin relaxation times,[29, 30] show the same kind of accelerating deviation from simple liquid behavior as the liquid is cooled far from the glass transition temperature.

Another surprising characteristic of water is its preferential orientation in the hydration shell of nonpolar solutes and nonpolar side groups attached to biopolymers. The structure adopted by liquid water which is in close proximity to nonpolar solutes is a fundamental characteristic of modern theories of hydrophobic hydration and hydrophobic effects, which are of great relevance to our understanding of many important chemical and biological processes.[31]

Placing a solute molecule in liquid water leads to a rearrangement of the random H-bond network. Besides making some space for the guest molecule, water tries to strengthen its network around the nonpolar solute. This can best be done by placing its tetrahedral bonding directions in a straddling mode[32] as shown in Figure 4 (left). The water

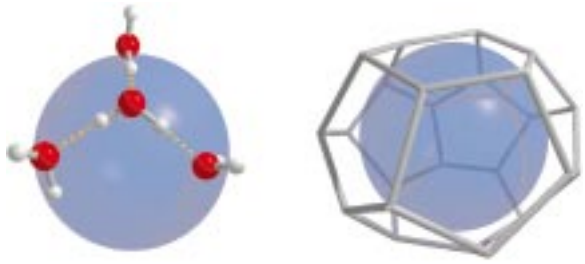

Figure 4. Water molecules next to a nonpolar solute. Each water molecule prefers to place its tetrahedral bonding directions in a straddling mode (left). A possible full arrangement of such a H-bonded network is shown for a crystal structure of a clathrate hydrate (right).

molecule is aligned with three tetrahedral directions tangential to the surface of the occupied space in order to preserve the maximum number of H-bonds. This orientational restraint leads to a negative entropy contribution for the solution. The crystal structures of the clathrate hydrates of many nonpolar substances show that such arrangements are possible in principle (Figure 4 (right)).

3. Hydrogen Bonds and their Arrangements

3.1. Structure and Properties of the Water Molecule

Qualitatively, insight into the origin of these peculiar liquid properties is available from a consideration of the shape and bonding characteristics of the water molecule (Figure 5). A simple molecular orbital description provides a useful qualitative picture of the electron distribution in the water molecule. Four localized regions of excess charge appear in a tetrahedral arrangement around the central oxygen atom. Two positive regions are associated with the hydrogen atom

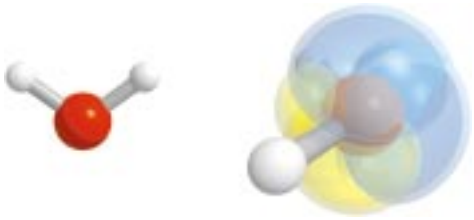

Figure 5. The water molecule (left). The two positive regions at the hydrogen atoms and the negative "lone pair" orbitals of the oxygen atom (right) obtained by an NBO analysis.

nuclei, which are significantly stripped of their attendant electrons by the highly electronegative oxygen atom.

The excess negative charge that thus appears around the oxygen atom is organized primarily in two lobes, or "lone-pair" orbitals, which complete the tetrahedral arrangement of the local electron deficit or excess. Overall, the electron distribution in an isolated water molecule can be related to the value of the equilibrium bond angle (104.5°), the value of the dipole moment (1.85 D), and the tetrahedral coordination of water molecules in condensed phases.[2]

3.2. Hydrogen Bonding in the Water Dimer

The intermolecular attraction between the hydrogen atom of one water molecule and the lone-pair electrons on another represents an H-bond. Hydrogen bonds are the dominant interactions between water molecules. Thus much experimental and theoretical effort has been directed toward understanding the nature of the water dimer, which represents the archetype for hydrogen bonding.

The water dimer (Figure 6) exists in the vapor phase and was measured for the first time by Dyke and co-workers.[33, 34] Their molecular beam resonance experiments clearly showed that the lowest energy arrangement has a plane of symmetry containing the hydrogen donor molecule to the right and the symmetry axis of the molecule to the left. As shown in following sections, experiments using advanced techniques as well as high-level quantum-mechanical calculations fully support the notion of linear H-bonds. The measured bond length in the water dimer of about 2.98 Å is significantly longer than the observed distances in both liquid water and regular ice (about 2.85 and 2.74 Å, respectively). The shortening of the $R(O\cdots O)$ distance in stronger H-bonded networks can be attributed to the cooperative nature of hydrogen bonding which will be discussed in detail in following chapters.

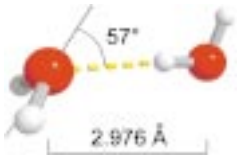

Figure 6. Experimental structure of the water dimer as measured from molecular beam resonance studies by Dyke et al.[33, 34] Covalent chemical bonds are shown as solid lines and H-bonds as dashed lines.

3.3. Tetrahedral Structures

The tetrahedral arrangement of the bonding groups in a single molecule results in the possibility of the molecule only forming four H-bonds with nearby molecules (Figure 7). In a so-called "Walrafen" pentamer,[35–40] the two hydrogen atoms of the centered molecule act as acceptors and the two lone pairs as donors. It is possible to fill three-dimensional space with tetrahedrally coordinate units, and some realization of this is the solid ice I_h crystal, which water forms on freezing at atmospheric pressure, as well as clathrate hydrates, which are described in detail in the next section. This possibility indicates that all microscopic and macroscopic properties arise from the fact that liquid water is a three-dimensional tetrahedral H-bonded (HB) network.

Figure 7. Tetrahedral configuration of water molecules spanned by two covalent bonds and two "lone pairs" of the central monomer.

3.4. Ice I_h and Ice Polymorphs

Thirteen crystalline phases are presently known: I_h (h = hexagonal), I_c (c = cubic), ice II – XI[41, 42] and XII.[43, 44] Two distinct amorphous water structures, low- and high-density amorphous ice, have also been reported.[8] This uncommonly large number of different solid phases attests to the structural versatility of the water molecule. Relative to ice I_h, all the other phases exist at lower temperatures and/or higher pressures. Those phases differ in the connectivity of the rings and in the position of the hydrogen atom between the oxygen atoms, and show bent H-bonds.[45] We will now take a closer look at ordinary hexagonal ice I_h, which is shown in Figure 8 along with cubic ice I_c. The oxygen atoms in ice I_h possess almost tetrahedral coordination. Each water molecule is involved in four H-bonds, with the two lone pairs as donors and both hydrogen atoms as acceptors. Compared to the gas-phase geometry, the distance $R(O\cdots O)$ is shortened to 2.74 Å and the bond length $R(O{-}H)$ is lengthened to 1.01 Å as a result of hydrogen bonding. Simultaneously, the intramolecular bond angle $\sphericalangle$(H-O-H) is widened to the typical tetrahedral angle of 109.5°. All these structural changes can be attributed to cooperative effects in hydrogen bonding. I_h and I_c are presented here

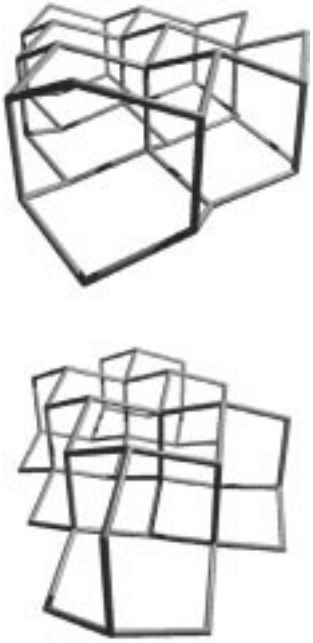

Figure 8. The structure of hexagonal ice I_h (top) and cubic ice I_c (bottom).

because of their structural motifs of chair- and boatlike hexamers, which play a significant role in the experimental and theoretical studies discussed later.

3.5. Clathrate Hydrates

Clathrate hydrates present the greatest variety and most intensively studied of H-bond inclusion compounds. The ability of water molecules to form a wide variety of four-coordinate networks, which results in the polymorphism of ice, is also apparent in the hydrate inclusion compounds. The voids in clathrate hydrates are much larger than in ice, and the H-bonded networks are unstable unless they are occupied by guest molecules. After the discovery of crystalline hydrates of chlorine by Davy[46] and Faraday[47] in 1823 it took more than a century before von Stackelberg and Müller[48] and Pauling and Marsh[49] could determine the structure of this chlorine hydrate and its gas hydrates. In the meantime the crystalline structures of the gas hydrates had been well characterized. Generally the structures are of the cagelike type-I or type-II clathrate structures. The structure-type formed depends upon the size of the guest gas molecule,[50] which stabilizes the lattice through nonbonding repulsive interactions.[51, 52] These structures have a pentagonal dodecahedron (5^{12}) of radius 3.9 Å as a principle building block. As this is not a space-filling polyhedron, the crystalline form of those hydrates contain a second larger polyhedra to form the lattice; that is a tetrakaidecahedral ($5^{12}6^2$) unit for type-I and a heccaidecahedral ($5^{12}6^4$) unit for type-II clathrates. All the principle building blocks are shown in Figure 9. Ripmeester and

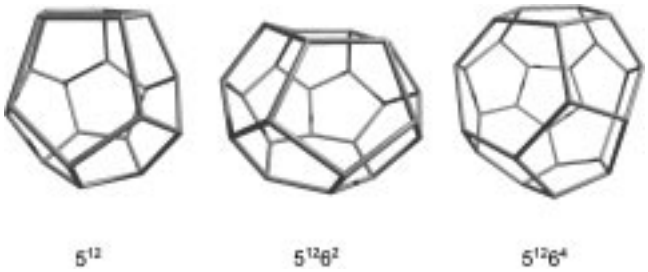

Figure 9. Clathrate structures of cage type I and II: dodechedron (5^{12}), tetracaidecahedron($5^{12}6^2$), and heccaidecahedron ($5^{12}6^4$).

Ratcliffe[53] used ^{129}Xe NMR spectroscopy to identify a new clathrate hydrate. An X-ray powder pattern diffraction study has shown this clathrate to have a host lattice isostructural with a known clathrasil structure, which contains the polyhedra 5^{12}, $4^3 5^6 6^3$, and a larger one, $5^{12}6^8$. More recently, Udachin and Ripmeester reported a complex clathrate hydrate structure showing bimodal guest hydration.[54] Formally this structure consists of alternating stacks of structure H and II hydrates, and might conceivably be found in those settings in which clathrate hydrates form naturally. The ubiquity of such motifs in crystalline hydrates led Pauling to formulate a "clathrate theory" of liquid water[55] that was built upon dodecahedral and tetrakaidecahedral clusters as structure units, but this picture has not received widespread support.

However, in a computer simulation study of the hydrogen-bond network, Geiger et al.[56] found some evidence for the existence of numerous clathrate-like holes in liquid water. The same shape of orientational distribution functions have been observed when studying the orientation of water molecules in the hydration shell of hydrophobic solutes.[32] Thus the structure was characterized as "clathrate-like", since the hydration shell molecules are oriented in such a way that one of the four tetrahedral bond directions points radially outward and the remaining three bonding directions straddle the dissolved particle (Figure 4 (left)).

The academic interest concerns the water–water interaction in these topologically rather complex systems and the guest–host interaction with guest species that range from noble gas atoms to large and polar organic molecules. Clathrates are also believed to occur in some outer planets at fairly high temperatures. The interest is, however, not only academic: The petrol industry suffers from the nuisance of hydrocarbon clathrates blocking gas pipelines in arctic regions, and has just started to show interest in the giant natural methane deposits in the deep ocean floor and in permafrost regions.[57, 58]

3.6. Statistical Networks

So far we have characterized some of the structures which occur in the gas phase of water or polymorphs of ice. The precise nature of the H-bonded disorder of water in the liquid phase is still unknown. Scattering experiments of liquid water give a precise description of atomic position disorder, but simply do not lead to a uniquely clear picture of the H-bonded network. Thus computer simulation methods, such as molecular dynamics (MD) or Monte Carlo (MC) simulations, are helpful for generating a representative set of configurations for a small region within the solid or liquid of interest. These calculations predict a totally connected random network of H-bonds as shown in Figure 10. The melting of ice results in a latent heat of 1.4 kcal mol^{-1} being absorbed. This value is equivalent to breaking about 10% of the H-bonds and the system becoming "frustrated". The water structure at any instant and on any length scale is amorphous, with many dangling bonds. Its structure becomes "random" and contains many five- and seven-membered rings, as well as the ice six-membered ring.[59, 60]

Figure 10. Statistical network of liquid water. Snapshot from molecular dynamics simulations.

4. Many-Body Effects/Cooperativity

The nature of the physical interaction that contributes to hydrogen bonding has been the subject of numerous discussions in the chemical literature.[61] On one side, H-bonds are attributed to purely electrostatic interactions, or to electrostatic plus polarization interactions; on the other side covalent interactions are considered to be extremely important. As discussed, there is increasing experimental evidence for the partial covalence of the H-bond. The more recent and prominent ones are the Compton scattering experiments on ice I_h by Isaac et al.[62, 63, 64] and NMR measurements of ^1H-^{15}N and ^{15}N-^{15}N scalar couplings of several H-bonded biological systems by Grzesiek et al.[65, 66] It should be noted that the covalent contributions to H-bonding concluded from Compton profiles is highly controversial. Parrinello et al.[67] calculated the same features of the electron distribution in ice I_h, but come to a different chemical interpretation.

Cooperativity of H-bonding in water was originally an idea of Frank and Wen.[68] The formation of a first H-bond (Figure 11) results in a change in the charge distribution

Figure 11. Hydrogen-bonded water dimer in the framework of an NBO analysis.[74] The overlap of an oxygen lone pair orbital and an antibonding OH orbital is shown.

within the participating monomer in such a way that the hydrogen acceptor molecules becomes potentially an even better H-bond donor than before. It is capable of forming a stronger second bond because of the existence of the first bond. The same is true for the proton donor, which has an enhanced ability to accept a proton as a result of the bond that it has already formed. This idea has been supported for many years by quantum mechanical studies. Kollman and co-workers used a Morokuma analysis[69, 70] of the results from an ab initio calculation to break down the interaction energy of the water dimer into four components: electrostatic, polarization, charge transfer, and dispersion. The authors found out that the contributions of various components varied with intermolecular distance. Roughly half the interaction at the equilibrium distance of about 2.98 Å could be attributed to electronic interactions.

Weinhold and co-workers performed a natural bond orbital (NBO) analysis to eliminate the charge-transfer component from the Hamiltonian operator of H-bonded dimers.[71] They reported that this component constituted the major energetic contribution to many H-bonds, whereas electrostatic attraction was largely canceled out by exchange repulsion. Thus, the interaction energy can be considered to be a consequence of a charge-transfer interaction. In this Lewis-type picture the donor–acceptor interaction between a lone pair on an oxygen atom and an O–H antibond leads to an energetic stabilization as a result of progressive charge transfer (CT).[72, 73] This CT interaction is responsible for both enthalpic and entropic factors that stabilize certain H-bond clusters over others. For example, the cooperative effects in a water pentamer (Figure 12) lead to H-bonding energies that are almost twice as

Figure 12. Overlapping of the oxygen lone pair orbital and the antibonding OH orbital in an equilibrium structure of the $(H_2O)_5$ pentamer. The average H-bond strength is almost twice that in the dimer as a result of cooperative effects.

strong as the linear dimer H-bond.[74, 75] Some of the consequences are: Strong CT interactions tend to lengthen the covalent O–H bond and to shorten the noncovalent H···O hydrogen bond, thus reducing the overall R(O···O) separation as given in Table 1. On enthalpic grounds, cooperative

Table 1. Calculated average distance R(O···O) and bond length R(O–H) [Å], NBO delocalization energies $\Delta E_{n\rightarrow n+1}$ [kcal mol^{-1}] from oligomer W_n to oligomer W_{n+1}, and natural charge transfer q_{CT} [e] in water clusters (RHF/6-31 + G*).[75]

	R(O···O)	R(O–H)	$\Delta E_{n\rightarrow n+1}$	q_{CT}
W_1	–	0.9476	–	–
W_2	2.964	0.9491	9.73	0.009560
W_3	2.872	0.9514	8.70	0.008917
W_4	2.847	0.9531	15.04	0.015397
W_5	2.837	0.9536	16.72	0.016404
W_6	2.833	0.9535	16.94	0.016673

bicoordinate ring structures are intrinsically favored over open-chain and starlike topologies (Figure 13). On entropic grounds, two-coordinate connectivities such as chains and cycles are favored over three- or four-coordinate networks. Compared with two-coordinate closed CT ring forms, higher three- and four-coordinate clusters are disfavored at higher temperature because of strongly hindered intermolecular bending or stretching modes. These reduce the librational entropy contributions and the unfavorable cooperative H-bond directionality patterns which lead to significant enthalpy loss. The occurrence of the three-dimensional structures at lower temperatures is caused by the high connectivity and the resulting larger total H-bond energy.

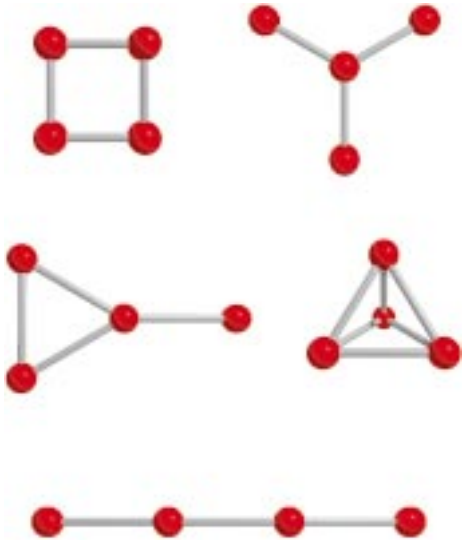

Figure 13. H-bond formations of water molecules: ring, star, lasso, tetrahedron, and chain.

5. Water Models

5.1. Mixtures Models

The combined importance and peculiarity of water has inspired scientists for more than a century to construct conceptual models which reproduce the observed behavior of the liquid. The earliest attempt probably goes back to Röntgen in 1892. He explained the density maximum as resulting from a shifting equilibrium between small ice crystallites suspended in a liquid of dissociated individual molecules.[76] Röntgen's concept was based on the idea that liquid water can be modeled by a mixture of two locally less- and more-dense structures. It thus represents the first of a family of so-called "mixture models" for the liquid structures.[77] Such models focus on the H-bond structures of the liquid and distinguish between a population of "intact" and "broken" H-bonds. This view was naively confirmed in infrared studies of liquid water.[78] A strong overtone of the OH stretching mode was found with two distinct components in the 1.4 to 1.6 μm region. The absorbance of the lower wavelength component decreases with decreasing temperature, while the higher wavelength component increases. This behavior has been associated with the expected decrease in the population of "broken" H-bonds as the liquid cools. Although other explanations do not require two distinct states of bonding, those experimental results encouraged several scientists to follow the idea of bonded and nonbonded structures for modeling the properties of liquid water.[79–81] Stanley and Teixeira[82] presented a more modern model in this spirit. Their statistical model does not require that water molecules are strictly H-bonded or not H-bonded; it simply describes the degree of connectivity that is observed to occur in a lattice of four-coordinate sites when some random fraction of the nearest neighbors are considered bonded, and the rest are considered unbound. The two groups of interacting water molecules are distinguished for example by an energetic criterion. It could be shown that clusters of four-bonded molecules will be observed as the probability of bonding to a nearest neighbor increases. The thermodynamic anomalies of water could be explained by considering those four-bonded clusters to be associated with regions of larger molecular volume, lower energy, and higher order. The authors results held when random configurations of molecular sites in the continuum, taken from computer simulations of water, were used.[83, 84]

5.2. Continuum Models

"Continuum models" contrast to the mixture models in that in the former it is considered that the H-bonds are never broken in the liquid, but are only more or less distorted from their optimal form. A more modern example is the "continuous random network" (CRN) model of Sceats and Rice.[85] This approach is supported by the observation that H-bonds need not necessarily break for molecules to have the mobility that is characteristic of the liquid. The model is based on continuous modifications of the topology of the H-bonded network rather than disruption of local H-bonded associates. This view implies there are "bifurcated" H-bonds or shared H-bonds between two atoms of one molecule.[86]

The picture of continuous modification of the H-bonded network has been proven useful in explaining the mobility of water molecules in the liquid.[87–89]

A distinction between mixtures and continuous models could be made as follows: in the former there are intact and broken H-bonds, while in the latter there is a fully H-bonded network. There is a continuous transition between these extremes. For example, the model of Stanley and Teixeira,[82] which is given above as a modern mixture model, can also be regarded as a continuous model. The introduction of a threshold for H-bonds into a continuous model picture leads to a mixture model.

6. Survey of Calculated Water Clusters

Semi-empirical and ab initio quantum mechanical studies on water clusters are numerous.[90–120] This development went along with improved methods and better computational capabilities. Our survey concentrates on recent ab initio Hartree–Fock (HF) and density functional (DFT) calculations. For clusters larger than $n = 30$, only semi-empirical calculations are taken into consideration. The presented water clusters are discussed as a function of size and connectivity so that most of them can play a significant role in the experimental and theoretical investigations described later.

6.1. Small Cyclic Water Clusters ($n = 3–6$)

The optimal structures and harmonic vibrational frequencies of small water clusters including ring structures W_n, $n = 3–6$, have been determined by Xantheas et al.[121–124] with

Hartree–Fock (HF) and density functional (DFT) methods, as well as Møller–Plesset second order perturbation theory (MP2) with an augmented correlation-consistent double-zeta basis set (Figure 14). The density functional B-LYP used

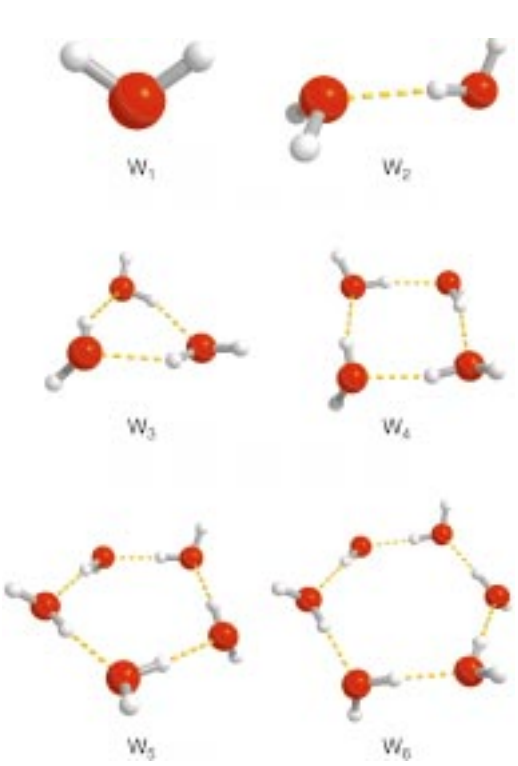

Figure 14. Small water clusters ($n=1-6$) as calculated by ab initio and DFT methods.[121]

combines the Becke's gradient-corrected exchange functional with the gradient-corrected correlation functional of Lee, Young, and Parr.[123] The authors were particularly interested in the correlation of various properties with cluster size. Thus they performed benchmark studies of the water monomer and H-bonded dimer to ascertain the minimum level of theory and basis set that would yield meaningful results for the larger clusters. Accurate structure, harmonic frequencies, dipole moments, and polarizability components for the water molecule, along with several measured properties for the water dimer, such as the structure and rotational constants, were chosen as benchmarks. The most important results concern the structural and spectral trends in small cyclic water clusters. The study of cyclic clusters ($n=3-6$) reveals a systematic contraction of the nearest $R(O\cdots O)$ separation with increasing size, a fact which can be attributed to nonpairwise additive (cooperative) many-body interactions as discussed earlier. As given in Table 2, the $R(O\cdots O)$ distance decreases nearly exponentially with increasing cluster size. The HF results, although not as accurate as the correlated data, exhibit the same trends as the DFT and MP2 results. While the $R(O\cdots O)$ separation decreases, the length of the bridged OH bonds increase monotonically with increasing ring size. The $R(O{-}H)$ bond length in the MP2 tetramer is about 2 pm longer than in the water monomer.

Table 2. Calculated average $R(O\cdots O)$ distances [Å] in water clusters W_n ($n=2-6$) at various levels of theory with the aug-cc-pVDZ basis set.[121–123]

Cluster	HF	B-LYP	MP2
W_2	3.032	2.939	2.911
W_3	2.927	2.808	2.799
W_4	2.880	2.743	2.743
W_5	2.867	2.727	–
W_6	2.855	2.714	–

The vibrational spectra of small water clusters ($n=4-6$) show a blue shift of about 70 cm^{-1} for the intramolecular bending mode with respect to the monomer. The corresponding red-shifts in the OH stretches were estimated to be about 50 and 500 cm^{-1} for the free and bridging hydrogen atoms, respectively, with respect to the monomer. These values are in excellent agreement with experimental observations both on small water clusters as well as the bulk, as we will see later. Xantheas et al. pointed out that geometries, harmonic frequencies, and IR intensities can provide guidance to research groups studying water clusters; they demonstrated that the shifts in the OH stretching frequencies correlate well with the changes in the corresponding equilibrium bond distances and obey the well-known Badger's rule.[125]

6.2. Isoenergetic Water Hexamer Clusters ($n=6$)

An accurate theoretical description of the water hexamer is an interesting and fundamental subject. The cyclic hexamer, as discussed above, is the building block of many ice forms and it appears to be relevant for liquid water as well.

Prompted by the surprising experimental results for the water hexamers in the gas phase, Kim and Kim[126] performed extensive ab initio and DFT calculations on the five lowest energy structures of the water hexamers (Figure 15). The authors demonstrated that the ring, book, bag, cage, and

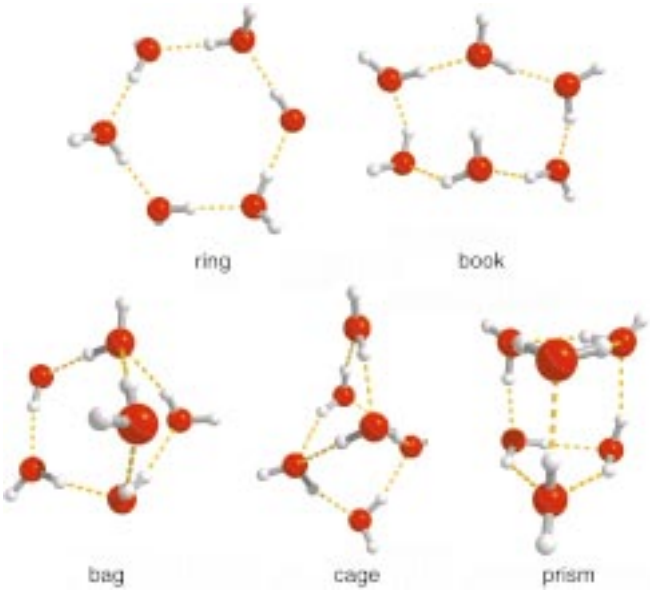

Figure 15. Calculated water hexamer isomers showing quasiplanar and cagelike clusters.[126]

prism structures have energies that are within 0.7 kcal mol^{-1} of each other, that is, they are nearly isoenergetic. Their MP2 calculations showed that the lowest energy conformer is the cage followed by the book (within 0.1 kcal mol^{-1}) and the prism structure (within 0.2 kcal mol^{-1}). The ring and the bag structures are only slightly higher in energy (0.5 and 0.7 kcal mol^{-1}, respectively) than the cage hexamer. The free energy of the book hexamer above 40 K is slightly lower than the cage, which might imply that the book structure would be more populated and thus be detectable. At higher temperatures the populations of the five hexamers would be almost the same. Deuteration did not change the nearly isoenergetic behavior of the clusters. The cage structure is still the lowest energy conformer, followed by the two competing structures of the book and the prism, whose energies are only 0.2 kcal mol^{-1} higher at 0 K. Above 55 K the book form would again be more populated than the cage structure. The nearly isoenergetic nature of the water hexamers suggests that the kind of structure that will be detected experimentally strongly depends on the physical and chemical environment.

6.3. Variety of Water Heptamers ($n = 7$)

In spite of a spate of studies of various water clusters, only a few theoretical investigations on the water heptamer are available. The experimental vibrational spectra of water heptamers encouraged Kim et al.[127] to perform ab initio and DFT calculations on twelve possible water heptamer structures to explore the conformations as well as the spectroscopic properties of these water clusters. Two three-dimensional cagelike structures comprised of a seven-membered ring with three additional H-bonds were found to be the lowest energy heptamer conformers (Figure 16). The global

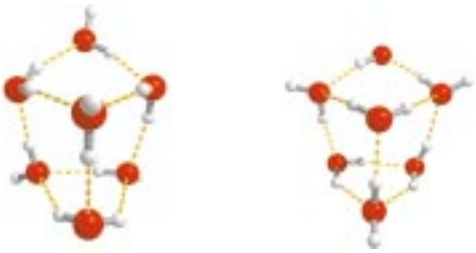

Figure 16. Energically low-lying isomers of calculated water heptamers.[127]

minimum energy of the most stable species was found to be 0.5 kcal mol^{-1} lower than the other. The Gibbs free energy calculations using HF and B3LYP frequencies have shown that both structures are stable up to 100 K. An almost two-dimensional ring conformer lies only 1 kcal mol^{-1} above the global minimum at 0 K. Above 150 K, this ring structure is more stabilized than the three-dimensional heptamers for entropic reasons. The vibrational spectra of different heptamer conformers were discussed and compared with spectra of the hexamer and octamer water clusters.

6.4. Water Octamers: Cubic or Cyclic?

Some of the forementioned water heptamers can be generated from the two most important water octamer conformers. These cube water structures with D_{2d} and S_4 symmetry present isoenergetic global minima.[128] They contain two kinds of water monomer: donor-donor-acceptor and acceptor-acceptor-donor molecules. Both cubic octamers are shown in Figure 17 along with a nearly cyclic and a bicyclic

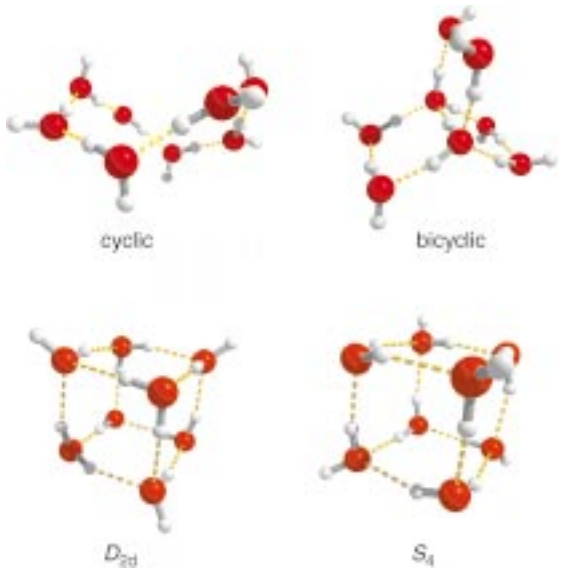

Figure 17. Cyclic, bicyclic, and cubic octamers of water obtained from ab initio calculations.[128, 129]

octamer calculated by Weinhold.[129] The cyclic topology has less H-bonds than the polycyclic octamers (8 versus 12) and is thus energetically disfavored. Its strong thermodynamic stability is caused by entropic factors. A virtually free torsion about the H-bond axis in the cyclic octamer leads to lowest frequency vibrations whereas angular strain factors in the cubic structures cause higher vibrational temperatures of the lowest H-bond modes.[129]

6.5. Ice-Like and Clathrate-Like Structures ($n = 12 - 26$)

Larger water clusters with up to 26 water molecules were calculated by Ludwig and Weinhold.[130] The species W_{12}, W_{18}, and W_{26} (Figure 18) were chosen as representative clusters with hexagonal units. Those hexagonal facets are well known structural elements of known crystallographic ice forms.[42] The W_{12} cluster has two W_6 rings directly coupled face to face in a charge-balanced fashion, with each vertex (oxygen atom) having trigonal coordination. A more ice-like fragment is the W_{18} cluster, which contains an adamantane-like core buttressed with three W_2 side chains. Although this polycyclic cluster exhibits hexagonal elements of a tetrahedral lattice, it has no four-coordinate vertices that could truly resemble a typical interior site of bulk ice I_h. The W_{26} cluster was initially formulated as a tetrahedral diamond-like microcrystal with central water molecules concentrically surrounded by succes-

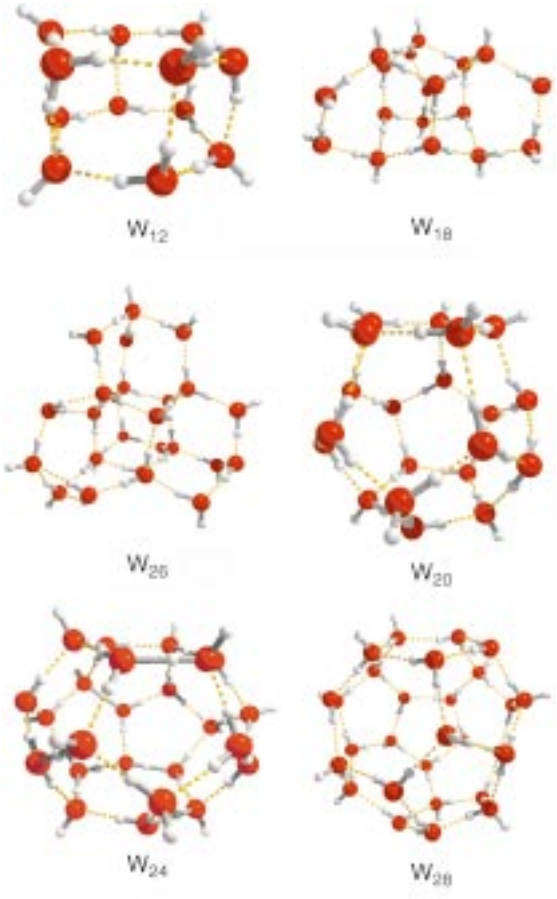

Figure 18. Ice- and clathrate-like water clusters.[130]

sive shells of tetrahedral coordination to give increased numbers of "interior" four-coordinate monomers at each shell. However, even the W_{26} cluster contains only six four-coordinate (plus eight three-coordinate and twelve two-coordinate) monomers, which leads to an average coordination number of 2.77. This value is less than in the trigonal coordination of the fullerene-like topologies W_{20}, W_{24}, and W_{28} (bucky water). While pentagonal and hexagonal facets are well-known structural elements of crystallographic ice forms,[42] the intact bucky-water polyhedra are principally recognized as crystallographic elements in certain clathrate-type hydrates, such as the pentagonal dodecahedral (5^{12}), tetrakaidecahedral ($5^{12}6^2$), and the hekkaidecahedral ($5^{12}6^4$) units. The large number of calculated clusters are topologically similar; they differ only in the proton ordering around each vertex. The most stable species of the cage types are shown in Figure 18. The comparable tetrakaidecahedral cluster structures W_{24}, W_{25}, and W_{26} were also calculated by Khan.[131] He used semi-empirical methods for his calculations and described the structural features and stability of these clusters.

Most recently, Khan calculated multiple-cage clusters to examine whether these fused structure formations became more favorable as the cluster-size increases.[132] Indeed, the 35-mers having two fused dodecahedral cages consistently show a greater stability than their single-cage isomers.

6.6. Larger Clusters: Icosahedral Networks ($n = 280$)

Chaplin[133] formed an icosahedral three-dimensional network of 280 hydrogen-bonded water molecules. In this structure each water molecule is involved in four H-bonds, two as donors and two as acceptors. The network is based on the regular arrangement of 20 slightly flattened tetrahedral 14-molecule units as shown in Figure 19. Within these units

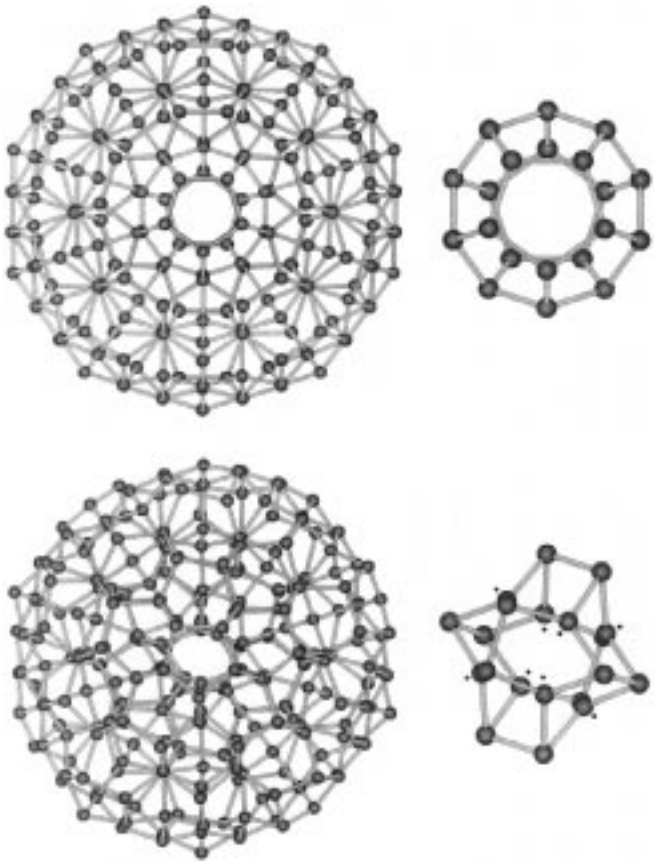

Figure 19. An expanded icosahedral water cluster consisting of 280 water molecules with a central dodecahedron (top) and the same structure collapsed into a puckered central dodecahedron (bottom). The figure is reproduced with the kind permission of Elsevier Science and M. F. Chaplin. [133]

four water molecules form the corners of the tetrahedron and are involved in both boat-form hexamers and pentamers. The remaining ten molecules form an adamantane-type ring structure, identical to a 10-molecule unit recently found in a crystalline supramolecular complex,[134] and also as found within the 18-molecule cubic ice cell. Four of these molecules are involved in hexamers in both the boat and chair conformation, with the remaining six molecules form pentamers and hexamers in the chair conformation.

Pentamers of water have bond angles of 108°, which are 1.47° closer to the supposedly most stable ∢(H-O-H) angle in water vapor (104.52°) than are the tetrahedral angles (109.47°) in ice. The clusters can grow in three dimensions; each cluster has twelve potential sites at its icosahedral vertices for use as centers for neighboring, overlapping clusters. The structure becomes more distorted as the network grows.

7. Survey of Measured Water Clusters

7.1. Small Cyclic Water Clusters ($n = 3-6$)

Enormous progress in laser spectroscopy has facilitated new, highly detailed studies of water clusters. Studies of the structure and dynamics of isolated small clusters of water molecules provide a means of quantifying the intermolecular forces and hydrogen-bonded rearrangements that occur in condensed phases. Far-infrared (FIR) vibration-rotation-tunneling (VRT) spectroscopy of clusters has recently been developed by Saykally and co-workers[135–145] to address such questions. Low-frequency van der Waals vibrations in clusters can be measured with tunable FIR lasers to resolve rotational and tunneling motions. The resulting VRT spectra can be analyzed in terms of permutation-inversion (PI) group theory and scattering theory to yield pair potentials of unprecedented accuracy and detail for weakly bonded systems. FIR-VRT spectroscopy is also a powerful probe of the tunneling dynamics that occur in hydrogen-bonded clusters. This method should allow for the investigation of the cooperative (nonpairwise) effects of hydrogen bonding in water clusters. In a series of beautiful experiments Saykally and co-workers characterized the water dimer,[135] the cyclic water trimer,[136] the tetramer,[137] and the pentamer.[138] The results unambiguously established that the structures of the water clusters responsible for the observed spectra were indeed the quasi-planar rings predicted by theory.[139] These spectra permitted estimates of the $R(O\cdots O)$ distances to be determined for each of the clusters and yielded a quantitative experimental measure of the hydrogen-bond cooperativity. The $R(O\cdots O)$ distance obtained from VRT spectroscopy and theoretical studies of water clusters are plotted in Figure 20. Consistent

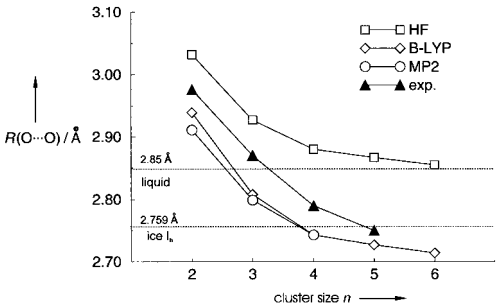

Figure 20. The $R(O\cdots O)$ distance versus cluster size obtained from VRT spectroscopy[136–139] and three different levels of theory: Hartree–Fock (HF), Møller–Plesset second-order perturbation theory (MP2), and density functional theory (B-LYP).[121–123] The experimental $R(O\cdots O)$ distances in liquid water at 298 K[155] and hexagonal ice I_h at 183 K[41, 42] are given for comparison and are indicated by dotted lines.

with the occurrence of cooperative effects, all the methods produced an exponential contraction of the $R(O\cdots O)$ distance with increasing cluster size which converged to the bulk (ordered ice) value of about 2.74 Å. Experiment and theory strongly suggest that the water trimer, tetramer, and pentamer have cyclic, quasi-planar minimum energy structures. Larger water clusters were expected to have three-dimensional geometries, with the hexamer representing the transition from a cyclic to a three-dimensional structure.

7.2. Water Hexamers: Cage, Quasiplanar Ring, or Chair?

7.2.1. The Cagelike Hexamer in the Gas Phase

As discussed in Section 6, ab initio studies on the hexamer reveal the existence of several low-lying structures, but predict that the minimum-energy form is the three-dimensional cage shown in Figure 21. This cagelike hexamer agrees best with

Figure 21. Experimentally found water hexamers: the cage structure detected in the gas phase,[146] the quasi-planar cyclic structure trapped in liquid helium,[147] and the chairlike cyclic structure measured in organic hosts.[148]

the measured rotational constants from VRT measurements performed by the Saykally group.[146] The fact that both high-level ab initio calculations and diffusion quantum Monte Carlo (DQMC) results[147–149] predict the cage as the lowest energy form, and that no structures other than the most stable have ever been detected by VRT spectroscopy in super-sonic argon jets, is fairly compelling evidence that the cage form is indeed the most stable water hexamer. Clearly the water molecules have enough time to find the absolute minimum structure in these gas-phase experiments at 5 K. Ab initio studies also predict that zero-point vibrational effects are crucial for the stability and that they can alter the energy ordering of the low-lying hexamer structures. Thus, there were some hints that other hexamer isomers could be detected by changing the chemical environment and temperature.

7.2.2. Quasiplanar Hexamers in Liquid Helium

Nauta and Miller recently reported the experimental observation of the cyclic water hexamer, which was a higher energy isomer than Saykally's cage structure previously characterized in the gas phase.[150] The ring hexamer shown in Figure 21 was formed in liquid helium droplets and studied by infrared spectroscopy. Three main results of this beautiful study are remarkable. Firstly, this isomer is formed selectively as a result of unique cluster-growth processes in liquid helium. The experimental results indicate that the cyclic hexamer is formed by insertion of water molecules into smaller, preformed cyclic complexes such as trimers,[151] tetramers, and pentamers. Buck and co-workers[152] obtained different results for growing methanol clusters in helium. Once the cyclic trimer was formed and cooled, insertion of the fourth methanol molecule into the ring was inhibited by the lack of energy needed to open the ring. The result was a tetramer structure corresponding to a cyclic trimer with the fourth molecule hydrogen bonded to the outside. As a possible

explanation for the difference between the water and methanol systems Nauta and Miller suggested that insertion into the water ring is facilitated by tunneling of the hydrogen atoms through associated barriers. In contrast, ring insertion may be inhibited in methanol because it involves more motion of heavy atoms. Secondly, the infrared spectrum for the OH stretches of water clusters formed in liquid helium were compared with those of the corresponding complexes formed in a free jet expansion experiment. The vibrational frequency shifts resulting from the interaction with the helium were negligible and the bonds for the dimer, trimer, tetramer, and pentamer essentially coincidence with the gas-phase bands.[153] An additional peak red-shifted relative to the pentamer was assigned to the cyclic isomer of the water hexamer. The most compelling support for this assignment comes from comparing the frequency shifts for all of these cyclic complexes with the corresponding ab initio and DFT calculations on the clusters (Figure 22). As already shown for intra- and intermolecular geometries, the frequency shifts vary smoothly with

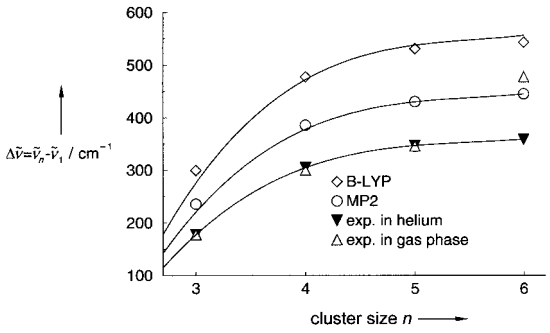

Figure 22. Experimental[150, 153] and calculated[121–123] red-shifts of the OH vibrational frequency for cyclic water clusters from the trimer to the hexamer. The shifts are taken in both cases relative to the average of the symmetric and asymmetric OH stretches of the monomer. The frequency shifts are essentially the same for the gas-phase and liquid helium data up to the pentamer. The band for the cage hexamer detected in the gas phase is more red-shifted than that of the hexamer in liquid helium relative to a quasi-planar ring structure. The solid curves present guidelines for the eye. They are obtained by scaling the fitted experimental curve to the theoretical data.

cluster size. The cyclic hexamer peak is precisely where it is expected theoretically, whereas the cage band is shifted further to the red region. Better agreement with experimental and theoretical values can not be expected given that the theoretical values are based on harmonic frequency calculations. From a theoretical viewpoint it is important that the calculated shifts can be scaled to the experimental data by one scaling factor for all cyclic clusters. Increasing cluster sizes clearly do not require different scaling factors. Thirdly, Nauta and Miller used superfluid liquid helium as a growth medium to access a different portion of the energy surface as in the gas-phase experiment, and could observe the cyclic water hexamer. This species is one of the prominent morphologies found in computer simulations of liquid water[60] and is the structural motif of ice I_h.[41, 42] The cage isomer characterized previously by Saykally and co-workers[146] has a most intense OH vibrational band which has a much greater red-shift. Several calculated local minima[126] lie lower in energy than the cyclic hexamer. Clearly the path between this hexamer and the three-dimensional cage structure will involve a great deal of H-bond rearrangement, which is expected to be difficult in liquid helium.

7.2.3. The Chairlike Hexamer in Organic Matrices

Recently, the supramolecular association of cyclic water hexamers with an ice-like chair conformer into one-dimensional chains inside an inclusion organic host was reported.[154] The geometric parameters of the hexamers are summarized in Table 3. The average $R(O\cdots O)$ distance of 2.776 Å is about the same as the analogous value of 2.759 Å in ice I_h at 183 K.

Table 3. Experimentally determined distances [Å] and angles [°] for water hexamers detected in an organic host.[154]

R(O – H)	R(O ··· O)	R(H ··· O)	∢O-H ··· O	∢O ··· O ··· O
0.960	2.711	1.758	171.3	113.2
0.956	2.785	1.844	167.6	96.0
1.264	2.833	1.703	145.0	140.2

However, there is a wide variation of the angles ∢(O-O-O); the average value is 116.5°, which is considerably deviated from the corresponding value of 109.3° which occurs in hexagonal ice. The hexamers are self-assembled by O–H ··· O H-bonds into extended chains along the channels, which consist of fused four- and six-membered water rings. The observed interhexamer oxygen – oxygen distance of 2.854 Å is very similar to the separation of 2.85 Å found in liquid water.[155] This supramolecular association of water molecules in chains is presumably enforced by the shape of the host's channels, whose relatively narrow openings preclude the formation of the more stable three-dimensional clusters found in the gas phase. There are no O–H ··· N H-bonds between the water chains and the organic host. Thus the water clusters can be removed by heating without changing the structure of the host. In contrast to previously described inclusion complexes of water clusters that have strong interactions with the host, the water clusters more closely resemble structures found in liquid water or ice. The IR spectra suggest that the water chains have more similarities with liquid water than with hexagonal ice.

Ice-like clusters with chair and boat conformations were also observed by Barbour et al.[134, 156] in the solid state. The intervening voids of a cobalt cage complex are filled with clusters of ten water molecules that adopt an ice-like conformation. The water cluster is sufficiently flexible to respond to small changes in its environment, but the overall conformation is robust.

However, free chair- or boatlike hexamers can not be detected. It clearly requires neighbors in a periodic system such as are present in hexagonal and cubic ice or organic matrices.

7.3. From Heptamers to Decamers

The understanding of the evolution of clusters larger than hexamers in the "cage" regime was the challenge of Buck and

co-workers.[157–159] Prior to their measurements, experimental results focused on the OH stretch of large clusters without size selection[160, 161] and $n = 7,8$ clusters attached to benzene.[162–164] Recently, Buck et al. presented the first infrared measurements of the OH stretch mode of pure water clusters with size $n = 7 - 10$. Their experimental method is a combination of size selection (by momentum transfer in collisions with rare gas atoms) with an infrared depletion technique.[165] In the first step the different clusters are dispersed into different angles according to their masses and detected by a mass spectrometer. Then the OH stretch vibrational mode of the water molecules is excited by IR laser radiation. The detector records the depletion in the cluster signal caused by dissociation of the clusters by the absorbed radiation. Additional calculations on the heptamers resulted in numerous energy minima, which can be divided into two structural families. The experimental spectra are reproduced quite well using the lowest energy structures similar to those found by Kim et al.[127] and shown in Figure 16. Inclusion of the zero-point motion effects was crucial for reproducing the spectra. The spectra of the two lowest isomers can be derived from the cubic S_4 octamer by removal of either one double donor or one double acceptor water molecule. The two cubic octamer isomers with D_{2d} and S_4 symmetry were characterized, along with nonamers and decamers, earlier by Buck et al.[157] using the same experimental method. The proposed lowest energy nonamer and decamer structures (Figure 23) are derived from

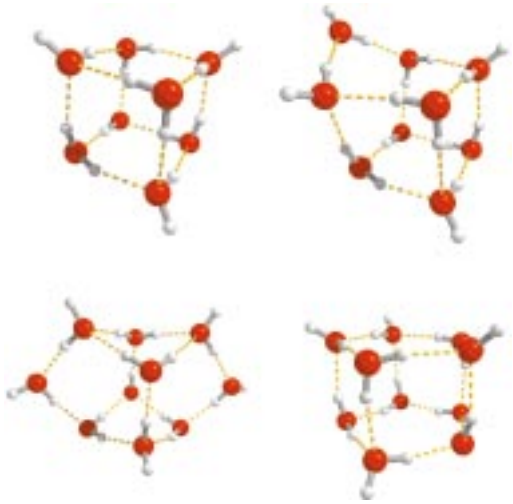

Figure 23. Structures of water clusters ($n = 8 - 10$): one cubic octamer (top left), one nonamer (top right), and two decamers (bottom) as measured by IR depletion techniques.[157–159]

the octamers by insertion of one and two two-coordinate molecules, respectively, into the cube edges. The two lowest energy decamers can be viewed as two fused pentamers with the same and the opposite orientation of H-bonds in the two cycles, respectively. However, the spectrum calculated for these two minima did not match the experiment very well. A better agreement was obtained for another "butterfly" minimum structure, which can be viewed as a D_{2d} octamer with two extra two-coordinate donor – acceptor molecules inserted at opposite edges.

The authors reported that the presented experimental technique will allow the measurements to be extended down to cluster sizes of $n = 6$ and up to $n = 20$ by changing the carrier gas and the collision partner.

8. Cluster Models for Liquid Water

8.1. Quantum Cluster Equilibrium Theory of Liquid Water

Weinhold[129] developed a method for calculating equilibrium properties of liquids by extending the standard statistical thermodynamic treatment of chemical equilibria to the analogous equilibria between molecular clusters, as characterized by modern ab initio techniques. The quantum cluster equilibrium (QCE) theory of liquids is based on the role of H-bonded molecular clusters as fundamental constituent units. Standard quantum statistical thermodynamic methods are used to treat the equilibria between clusters in the canonical ensemble, which leads to predictions of macroscopic thermodynamic and spectroscopic properties. Meanwhile QCE has been shown to provide practical, quantitative, or semiquantitative descriptions of H-bonded fluids such as amides[166–169] and alcohols.[170–173] The quantum cluster equilibrium formalism was first applied to the most important H-bonded fluid, namely, liquid water. In these first papers, emphasis was not placed on achieving high quantitative accuracy, but rather to illustrate qualitatively how the QCE model "works", and included the interplay between microscopic water clusters and macroscopic phase behavior, the stability of QCE predictions with respect to changes in the theoretical model or inclusion of other clusters, and the importance of nonpairwise additive cooperative effects in aqueous condensation phenomena. The simple seven-cluster QCE(7)/3-21G model for liquid water comprised clusters from the water monomers W_1 up to the cyclic n-mers W_5, W_6, and W_8.

It could be shown that structures found in the gas-phase experiments, such as the cubic octamer with D_{2h} symmetry are completely negligible in the QCE population, even though they are lower in energy. The reason for these dramatic differences in thermodynamic stability can be traced to energetic and entropic factors. The H-bonds in the cubic clusters are much more highly strained by the severe nonlinear O-H-O angles required along the cube edges, since the ideal 90° angle at each corner is much smaller than the equilibrium H-O-H bond angle. Severe angular strain in polycyclic octamers lead to higher vibrational temperatures of the lowest H-bond modes and result in much larger unfavorable entropic contributions. Such a process renders this species essentially irrelevant for describing equilibrium properties of water.

The QCE liquid-phase population as shown in Figure 24 consists mainly of cyclic octamers W_8. The next highest concentration of clusters are W_5 and W_6. Thus the equilibrium liquid phase is pictured as a mobile distribution of ring isomers that are packed roughly with van der Waals contact separation. This packing leads to characteristic near neighbor

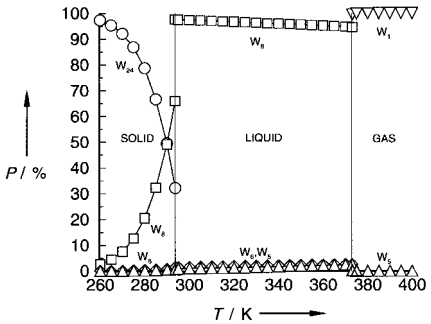

Figure 24. Cluster population P [mass %] from QCE(18)/3-21G model water at one atmosphere of pressure. The contributions of leading clusters are shown in each phase: W_{24}, W_8, and W_6 in the solid phase, W_8, W_6, and W_5 in the liquid phase, and W_1 and W_5 in the gas phase.[130]

$R(O\cdots O)$ distances of about 2.8 Å within the rings and a next-nearest $O\cdots O$ separation of about 4.5 Å. These values are crudely consistent with known features of the radial distribution function of liquid water. What is certainly not in agreement is the low number of nearest neighbors compared to the experimentally found number of 4.4. Also most of the thermodynamic properties, such as the liquid–vapor coexistence curve and heats of vaporization, could be reproduced in reasonable agreement. It was more difficult to reproduce a liquid–solid(ice) phase transition; for that it was necessary to calculate three-dimensional four-coordinate water structures similar to crystalline ice. Thus Ludwig and Weinhold[130] extended the QCE model of liquid water to include larger ice-like clusters, such as the tetrahedral and fullerene-like clusters with up to 26 water molecules. A low-energy tetrakaidecahedral W_{24} cluster (Figure 18) leads to a new low-temperature phase that borders on both liquid and vapor regions in first-order transition lines and gives rise to a true QCE triple point (Figure 25). The authors characterized

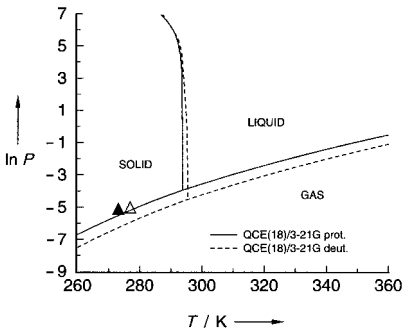

Figure 25. Phase diagram of the light and heavy QCE(18)/3-21G model water. The available experimental triple points for light (▲) and heavy (△) water are given for comparison.[130]

the microstructural composition and macroscopic properties of this "bucky ice" phase. Although it differs significantly from physical ice I_h (for example, the melting point is 20 K too high and the molar volume is 5% too low), it manifests qualitatively correct thermodynamic features of true ice polymorphs, which suggests an important role of voluminous clusters in the liquid/solid transition region. In further studies Ludwig and Weinhold extended the QCE theory to deuterated[174] and recently to tritiated[175] water clusters. They characterized the microstructural composition and macroscopic properties relative to those obtained for protonated species. The main goal was to compare the phase diagrams and thermodynamic properties of isotopically substituted water. It was found that the QCE triple point is shifted to higher temperatures by about 2.0 K upon deuteration and by about 3.0 K upon tritiation compared to the measured 3.8 K in heavy and 4.5 K in super-heavy water. The shifts of the melting point to higher temperature is also modeled correctly. The QCE theory allows for a change in the properties of light, heavy, and super-heavy water clusters (masses, momentum of inertia, zero-point energies, and vibrational frequencies) individually and/or in any combination. In this way the influence of different properties on cluster populations can be investigated. An interesting result is that the shift of the triple point to higher temperatures is a net effect: Lower zero-point energies for deuterated and tritiated water alone strongly raise the melting points, whereas a reduction in the vibrational frequencies for the isotopically substituted species alone lowers the melting point. The combination of the opposite effects result in a small net shift of the melting point to higher temperatures as shown in Figure 26. The larger masses and rotational temperatures in heavy and super-heavy water clusters have practically no effect on the melting point.

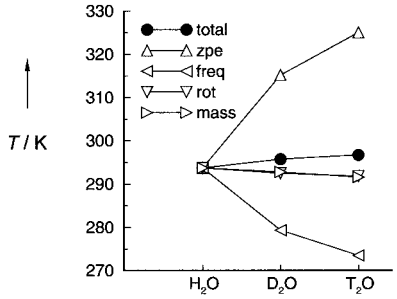

Figure 26. Calculated QCE triple points (●) for light, heavy, and super-heavy model water. The partial triple points are obtained by individually replacing zero-point energies (zpe), vibrational frequencies (freq), translational masses (mass), and rotational temperatures (rot).[175]

It is also interesting to note that isotopic substitution leads to different cluster populations in the liquid range. The dominant cyclic octamers W_8 are slightly replaced by W_5 and W_6 ring structures. It is usually assumed that shifts in thermodynamic and dynamic properties in going from H_2O to T_2O can be ascribed to zero-point-energy-induced thermal offset and keep the structural properties nearly identical.

8.2. Icosahedral Networks—A Structure Proposal for Water

Chaplin[133] proposed a fluctuating network of water molecules with localized icosahedral symmetry to explain many of the anomalous properties of water. This structure is built up from a mixture of hexamer and pentamer rings and contains cavities capable of enclosing small solutes. The model was developed by arranging alternating sheets of boat

and chair conformations of water hexamers from the lattices of hexagonal and cubic ice. This structure was folded to form an icosahedral three-dimensional network with capacious pores that is capable of partial collapse as a result of competition between the formation and destruction of H-bonded interactions. The stability of the network is balanced; it is able to fluctuate between an expanded low-density one of about 0.94 g cm^{-3} (Figure 19 (top)) and a denser collapsed one of about 1.00 g cm^{-3} (Figure 19 (bottom)) without breaking any H-bonds during the small changes that occur in the H-bond strength relative to the nonbonded interactions. The expanded structure is formed when structuring solutes or surface interactions are present which result in stronger H-bonds. Weak H-bonds yield the partially collapsed structure as a consequence of the formation of puckered dodecahedra. The resulting densities of both structures as given above can be related to well-known measured densities. The lower density structure may be compared with that of low-density water found around macromolecules[176] (0.96 gcm^{-3}), of supercooled water (-45°; 0.94 g cm^{-3}), and of low-density amorphous ice (0.94 g cm^{-3}).[177, 178] The high-density structure compares with the density of water at 273 K (1.00 g cm^{-3}). The collapse of all dodecahedral structures gives a density of 1.18 g cm^{-3}, which is similar to that of high-density amorphous ice at 1.17 g cm^{-3}.[178]

The structures allow the explanation of many of the anomalous properties of water, such as its density maximum as a function of temperature, and the viscosity minimum as a function of pressure. Additionally, the radial distribution pattern, the presence of both pentamers and hexamers, the change in properties and the "two-state" model of supercooling, as well as the solvation properties of ions, hydrophobic molecules, carbohydrates, and macromolecules can be reproduced.

The strongest direct evidence for this model is the agreement with the radial distribution functions. The high-density structure showed comparable radial distribution functions with that from X-ray[179] and neutron scattering[156, 180] data. As shown in Figure 27 there is a peak maximum at 2.8 Å. The

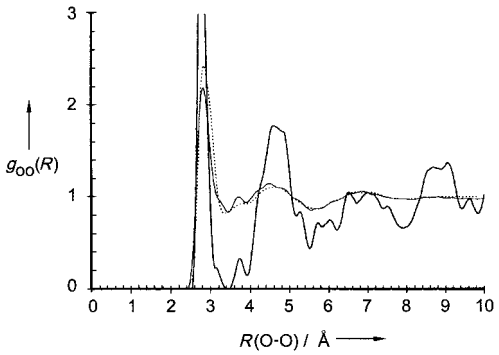

Figure 27. Comparison of the calculated radial distribution function $g_{oo}(R)$ of the high-density structure (——) with the X-ray diffraction data of water[179] at 277 K (——). The X-ray data yield a weighted sum of all atom pair distribution functions, which is mainly determined by the O···O contribution. The model peaks have been broadened by using a normal distribution with a standard deviation of 0.1 Å. The radial distribution function of oxygen atoms, as determined by neutron scattering,[156] is also shown (- - - -). The figure is reproduced with the kind permission of Elsevier Science and M. F. Chaplin.[133]

number of nearest neighbors of about 4.34 is also in good agreement with the reported 4.4 nearest neighbors calculated from diffraction data.[42] The radial distribution functions for the low-density structure can be compared with experimental data obtained for solutions, supercooled water, and the low-density amorphous ice. The distance between the cavities of 5.4 Å is close to the value of about 5.5 and 6 Å for supercooled water[56] and the Ne···Ne distance in water,[56] respectively. The radial distribution function of the low-density structure also shows similarities to those of the low-density amorphous structure. Both include features similar to cubic and hexagonal ices.[181] Neutron-diffraction data has been used to suggest the presence of pentamers, boat and chair conformers of hexamers, and partial dodecahedra.[182] By using Gaussian broadening for the high-density structure, the resulting four peaks at 2.8, 4.6, 6.7, and 9.0 Å show close agreement with the values of 2.79, 4.56, 6.95 and 8.60 Å measured by X-ray experiments.[183] The agreement with neutron scattering data[184] was even better.

8.3. A Simple Two-Structure Model for Liquid Water

A simple two-structure model for liquid water was proposed by Benson and Siebert.[185] The authors were able to construct a model involving isomerization between clusters which reproduces, within two per cent, the anomalous heat capacity of liquid water from the melting up to the boiling point. The clusters are polycyclic, cubic-shaped octamers which can dissociate into two cyclic tetramers. These clusters (Figure 28) are held together by H-bonds and although very

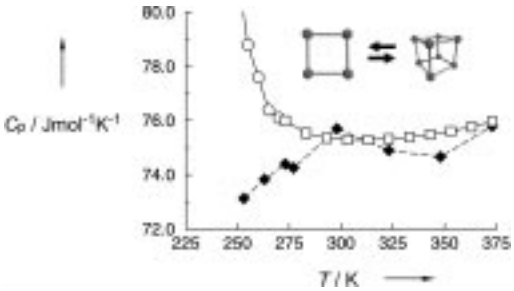

Figure 28. Heat capacity C_p of water as a function of temperature as calculated by Benson and Siebert[185] in comparison to measured data. The two-structure model includes tetramers and cubic octamers only.

labile, they appear to be the principal species present in liquid water according to this model. The fact that this two-structure model is capable of giving reasonable heat capacities is not too surprising. Structural theories of liquid water depend on the assumption that H-bonds can be considered as "intact" or "broken". Benson and Siebert fitted their model directly to bulk data, such as the sublimation energy of ice, the enthalpy of melting, and estimates of broken H-bonds. A satisfactory description of one or more of the properties of water over a particular range of temperature and density is usually obtained when an equilibrium of two species differing significantly in structural order and the number of H-bonds is used. As Benson and Siebert pointed out, the heat capacity

of water could also be obtained by assuming equilibria between polycyclic decamers and monocyclic pentamers. However, results from scattering experiments are not in agreement with the proposed structures.[186] If an $R(O\cdots O)$ distance of about 2.89 Å is assumed, then maxima in the pair correlation function should result at about 4.09 and 5.01 Å.[2] A maximum at 4.5 Å is found experimentally, which supports a tetrahedral structure.

Recently, Rodriguez et al. considered the water hexamer and octamer in a theoretical study of isomerization, melting, and polarity of model water clusters.[106] The model includes five hexamers of similar energy with different geometries and dipole moments, as well as two nonpolar octamers with D_{2d} and S_4 symmetry. The melting transitions were studied by using ab initio methods and empirical force field models. The melting transitions for the hexamer and the octamer were found at 50 and 160 K, respectively. The authors conclude that their results provide a comprehensive picture of the relationship that exists between the spatial and polarization fluctuations that occur in small water aggregates.

9. Summary and Outlook

Small water clusters and their properties can be calculated by high quality ab initio and DFT methods using extended basis sets. Most of the theoretical predictions for geometries and vibrational frequencies, as well as their behavior with increasing cluster size, are supported by experimental information. To the best of our knowledge these state of the art calculations are applied to clusters comprised of up to eight water molecules. For larger clusters Hartree–Fock calculations are performed on smaller basis sets. DFT is the method of choice for including electron correlation where post-Hartee–Fock methods are too expensive or impossible. These calculations are known for clusters with up to 30 water molecules. For most larger clusters, such as Chaplin's icosahedral water structures with 280 water molecules, only semiempirical methods can be applied. The problem with these methods is that H-bonds and their cooperative behavior are certainly not calculated in an appropriate way. Although calculations yield accurate structures and properties for small clusters, there remain shortcomings. Growing cluster sizes may lead to a dramatic increase in the number of isomers for each species which is no longer manageable. It requires a lot of experience and knowledge to pick out the plausible low-energy structures. The harmonic approximation is a further limit for calculating reasonable vibrational frequencies. The calculated frequencies are usually overestimated and corrected by a factor typical for the chosen method and basis set. It is some comfort that the measured trend of red-shifting of the OH stretch in water clusters can be smoothly reproduced by using only one correction factor. However, this is no longer true for low-lying frequency vibrations, which are particularly important for the use of calculated frequencies in the vibrational partition function. Another deficiency is the calculation of true minimum structures. Molecular dynamics and Monte Carlo simulations have shown that bifurcated structures may play a significant role in liquid water, particularly for describing its dynamics. These configurations are never present in low-lying minimum structures in ab initio calculations at 0 K.

The combination of calculated clusters and their properties with new laser spectroscopy experiments are likely to generate a wealth of information regarding the intricate details of how water molecules interact. Recent experiments have yielded detailed information about structural and dynamic aspects of small clusters. The clusters occur as nearly planar ring structures up to pentamers, whereas three-dimensional clusters are energetically favored with clusters larger than the pentamers. Large intermolecular zero-point energies of the H-bonds become crucial, and can alter the energy ordering of the low-lying hexamer structures. This is the reason why the cage hexamer is found in the gas phase and the quasi planar ring hexamer in liquid helium. The physical and chemical environment strongly determine the occurrence of different isomers. The geometries and vibrational frequencies have both been experimentally characterized up to the hexamer structures. The measured bond distances and vibrational frequencies provide strong support for the cooperative nature of hydrogen bonding. Growing cluster size, and thus increasing H-bond strength, lead to a shortage of intermolecular distances and a red-shift of the OH stretching modes as predicted by ab initio calculations. These findings certainly support theoretical predictions and experimental results that show the covalent character of hydrogen bonding.

Three water models based on the assumption that calculated molecular clusters and structures may be constituents of the liquid phase were recent presented. The quantum cluster equilibrium (QCE) model assumes that water species calculated from current ab initio methods are adequate representatives of the "flickering clusters" of the liquid-phase structure. This treatment of liquids is thus in the tradition of mixture models. The QCE model exhibits many characteristic features of a true gas/liquid phase transition (macroclustering, volume collapse, specific heat increase, Clausius–Clapeyron pressure dependence). The inclusion of larger ice- and fullerene-like clusters leads to a new low-temperature phase that bounds both liquid and vapor regions in first-order transition lines, and gives rise to a true triple point. Although the bucky-ice phase differs in significant respects from physical ice I_h, it manifests qualitatively correct thermodynamic features of true ice polymorphs, which suggests an important role of voluminous clusters in the liquid–solid transition. Nevertheless quantitative differences between theory and experiment currently remain. For example, the absence of a density maximum cannot be reproduced. The failure to accurately describe higher order temperature derivatives suggests the importance of incorporating vibrational anharmonic frequencies. Improved ab initio treatments of cluster–cluster interactions and molecular excluded-volume effects are also desirable. Although the current QCE model permits description of many interesting liquid properties at a useful level of chemical accuracy, rather high levels of theory as well as larger clusters may be necessary to achieve convergence to a quantitatively realistic water phase diagram.

Chaplin calculated large icosahedral structures, including 280 fully H-bonded molecules, to investigate long-range

ordering. This network can be converted between lower and higher density forms without breaking H-bonds. The structures allow explanation of many of the anomalous properties of water, such as its temperature – density and pressure – viscosity behavior, the radial distribution pattern, the presence of both pentamers and hexamers, the change in properties and the "two-state" model on supercooling, and the solvation properties of ions, hydrophobic molecules, carbohydrates, and macromolecules. As in the foregoing models, dynamic information is not obtainable. The calculation of dynamic properties is still the domain of molecular dynamics simulations.

Benson and Siebert could reproduce the anomalous heat capacity of liquid water from the melting to the boiling point by using a simple two-structure model. On the other hand, the proposed structures of a planar tetramer and a cubic octamer are certainly not suitable for describing the data obtained from X-ray and neutron scattering experiments of liquid water.

Among the proposed cluster models for water, QCE is the only unbiased approach. In the models of Chaplin and Benson discrete structures are proposed and their properties compared to those of liquid water. On the other hand, the QCE model yields equilibrium cluster populations as a result of quantum statistical calculations. Although the model does not give a continuously restructured random network, it does yield a hierarchy of species and structural motifs that may be important constituents of liquid water. Improving the quality of the calculated water clusters, as well as increasing their number and size, should permit an even better description of condensed-phase properties. However, there still remain certain limits to the capability of cluster-based approaches to understanding associated liquids in detail. Future theoretical and experimental investigations of larger water complexes showing new H-bond arrangements should ultimately enable a quantitative description of the complexity of the behavior liquid water to be made.

The author thanks A. Geiger, T. Farrar, and F. Weinhold for numerous discussions about the phenomena of water. Thanks are also due to A. Geiger and A. Benbow for carefully reading the manuscript. Financial support provided by the Deutsche Forschungsgemeinschaft and the Fonds der Chemischen Industrie is greatfully acknowledged.

Received: August 4, 2000 [A 425]

[1] N. E. Dorsey, *Properties of Ordinary Water Substance*, American Chemical Society Monograph, **1968** (facsimile of 1940 publication by Reinold Publ. Co).
[2] *Water—A Comprehensive Treatise*, *Vol. 1 – 7* (Ed.: F. Franks), Plenum, New York, **1972 – 1982**.
[3] P. G. Debenedetti, *Metastable Liquids*, Princeton University Press, Princeton, **1996**.
[4] P. Ball, *H_2O: A Biography of Water*, Weidenfeld & Nicolson, London, **1999**.
[5] J. D. Bernal, R. H. Fowler, *J. Chem. Phys.* **1933**, *1*, 515 – 548.
[6] A. H. Narten, H. A. Levy, *Science* **1969**, *165*, 447 – 454.
[7] F. H. Stillinger, *Science* **1980**, *209*, 451 – 457.
[8] O. Mishima, H. E. Stanley, *Nature* **1998**, *396*, 329 – 335.
[9] J. P. Cowin, A. A. Tsekoras, M. J. Iedema, K. Wu, G. B. Ellison, *Nature* **1999**, *398*, 405 – 407.
[10] J. M. Ugalde, I. Alkorta, J. Elguero, *Angew. Chem.* **2000**, *112*, 733 – 737; *Angew. Chem. Int. Ed.* **2000**, *39*, 717 – 721.
[11] R. S. Smith, B. D. Kay, *Nature* **1999**, *398*, 788 – 791.
[12] F. W. Starr, M.-C. Bellissent-Funel, H. E. Stanley, *Phys. Rev. E* **1999**, *60*, 1084 – 1087.
[13] M. E. Tuckerman, D. Marx, M. L. Klein, M. Parrinello, *Science* **1997**, *275*, 817 – 820.
[14] D. Marx, M. E. Tuckerman, M. Parrinello, *Nature* **1999**, *397*, 601 – 604.
[15] G. Kell in *Water: A Comprehensive Treatise*, *Vol. 1* (Ed.: F. Franks), Plenum, New York, **1972**.
[16] R. A. Fine, F. J. Millero, *J. Chem. Phys.* **1973**, *59*, 5529 – 5536.
[17] C. A. Angell in *Water: A Comprehensive Treatise*, *Vol. 7* (Ed.: F. Franks), Plenum, New York, **1972**.
[18] B. V. Zheleznyi, *Russ. J. Phys. Chem.* **1969**, *43*, 1311.
[19] B. V. Zheleznyi, *Russ. J. Phys. Chem.* **1968**, *42*, 950 – 952.
[20] C. A. Angell, H. Kanno, *Science* **1976**, *193*, 1121 – 1122.
[21] K. K. Mon, N. W. Ashcroft, G. V. Chester, *Phys. Rev. B* **1979**, *19*, 5103 – 5122.
[22] R. J. Speedy, C. A. Angell, *J. Chem. Phys.* **1976**, *65*, 851 – 858.
[23] C. A. Angell, J. Shuppert, J. C. Tucker, *J. Chem. Phys.* **1973**, *77*, 3092 – 3099.
[24] C. A. Angell, M. Oguni, W. J. Sichina, *J. Chem. Phys.* **1982**, *86*, 998 – 1002.
[25] F. X. Prielmeier, E. W. Lang, R. J. Speedy, H.-D. Lüdemann, *Ber. Bunsen-Ges. Phys. Chem.* **1988**, *92*, 1111 – 1117.
[26] Y. A. Osipov, B. V. Zheleznyi, N. F. Bondarenko, *Zh. Fiz. Khim.* **1977**, *51*, 1264.
[27] D. Paschek, A. Geiger, *J. Phys. Chem. B* **1999**, *103*, 4139 – 4146.
[28] D. Bertolini, M. Cassettari, G. Salvetti, *J. Chem. Phys* **1982**, *76*, 3285 – 3290.
[29] E. Lang, H. D. Lüdemann, *Ber. Bunsen-Ges. Phys. Chem.* **1981**, *85*, 603 – 611.
[30] R. Ludwig, F. Weinhold, T. Farrar, *J. Chem. Phys.* **1995**, *103*, 6941 – 6950.
[31] W. Blokzij, J. B. E. N. Engberts, *Angew. Chem.* **1993**, *105*, 1610 – 1648; *Angew. Chem. Int. Ed. Engl.* **1993**, *32*, 1545 – 1573.
[32] A. Geiger, A. Rahman, F. H. Stillinger, *J. Chem. Phys.* **1979**, *70*, 263 – 276.
[33] T. R. Dyke, K. M. Mack, J. S. Muenter, *J. Chem. Phys.* **1977**, *66*, 498 – 510.
[34] J. A. Odutola, T. R. Dyke, *J. Chem. Phys.* **1980**, *72*, 5062 – 5070.
[35] G. E. Walrafen, *J. Chem. Phys.* **1964**, *40*, 3249 – 3256.
[36] G. E. Walrafen, *J. Chem. Phys.* **1967**, *47*, 114 – 126.
[37] W. B. Monosmith, G. E. Walrafen, *J. Chem. Phys.* **1984**, *81*, 669 – 674.
[38] G. E. Walrafen, M. S. Hokmabadi, W.-H. Yang, *J. Chem. Phys.* **1986**, *85*, 6964 – 6969.
[39] G. E. Walrafen, M. R. Fisher, M. S. Hokmabadi, W.-H. Yang, *J. Chem. Phys.* **1986**, *85*, 6970 – 6982.
[40] G. E. Walrafen, W.-H. Yang, Y. C. Chu, M. S. Hokmabadi, *J. Phys. Chem.* **1996**, *100*, 1381 – 1391.
[41] N. H. Fletcher, *The Chemical Physics of Ice*, Cambridge University Press, Cambridge, **1970**.
[42] D. Eisenberg, W. Kauzmann, *The Structure and Properties of Water*, Oxford University Press, Oxford, **1969**.
[43] C. Loban, J. J. Finney, W. F. Kuhs, *Nature* **1998**, *391*, 268 – 270.
[44] M. Koza, H. Schober, A. Tölle, F. Fujara, T. Hansen, *Nature* **1999**, *397*, 660 – 661.
[45] P. Loubeyre, R. LeToullec, E. Wolanin, M. Hanfland, D. Hausermann, *Nature* **1999**, *397*, 503 – 506.
[46] G. A. Jeffrey, *An Introduction to Hydrogen Bonding*, Oxford University Press, New York, **1997**, p. 160.
[47] M. Faraday, *J. Sci. Liter. Arts* **1823**, *15*, 71 – 90.
[48] M. von Stackelberg, H. R. Müller, *J. Chem. Phys.* **1951**, *19*, 1319 – 1320.
[49] L. Pauling, R. E. Mash, *Proc. Natl. Acad. Sci. USA* **1952**, *38*, 112 – 118.
[50] D. W. Davidson in *Water—A Comprehensive Treatise*, *Vol. 2* (Ed.: F. Franks), Plenum, New York, **1973**, p. 115.
[51] P. M. Rodger, *Mol. Simul.* **1990**, *5*, 315 – 328.

[52] H. Tanaka, K. Kiyohara, *J. Chem. Phys.* **1993**, *98*, 4098 – 4109.
[53] J. A. Ripmeester, C. I. Ratcliffe, *J. Chem. Phys.* **1990**, *94*, 8773 – 8776.
[54] K. A. Udachin, J. A. Ripmeester, *Nature* **1999**, *397*, 420 – 423.
[55] L. Pauling, *Nature of the Chemical Bond*, 3rd ed., Cornell University Press, Ithaca, **1960**, p. 473.
[56] A. Geiger, P. Mausbach, J. Schnitker, *Water and Aqueous Solutions*, Hilger, Bristol, **1986**, p. 15.
[57] E. D. Sloan, *Clathrate Hydrates of Natural Gases*, Marcel Dekker, New York, **1990**.
[58] G. R. Dickens, C. K. Paull, P. Wallace, *Nature* **1997**, *385*, 426 – 428.
[59] A. Rahman, F. H. Stillinger, *J. Chem. Phys.* **1971**, *55*, 3336 – 3359.
[60] A. Rahman, F. H. Stillinger, *J. Am. Chem. Soc.* **1973**, *95*, 7943 – 7948.
[61] J. J. Dannenberg, L. Haskamp, A. Masunov, *J. Phys. Chem. A* **1999**, *103*, 7083 – 7086.
[62] E. D. Isaacs, A Shukla, P. M. Platzman, R. D. Hamann, B. Barbiellini, C. A. Tulk, *Phys. Rev. Lett.* **1999**, *82*, 600 – 603.
[63] E. D. Isaacs, A Shukla, P. M. Platzman, R. D. Hamann, B. Barbiellini, C. A. Tulk, *Phys. Rev. Lett.* **1999**, *83*, 4445.
[64] T. W. Martin, Z. S. Derewenka, *Nat. Struct. Biol.* **1999**, *6*, 403 – 406.
[65] A. J. Dingley, S. Grzesiek, *J. Am. Chem. Soc.* **1998**, *120*, 8293 – 8297.
[66] F. Cordier, S. Grzesiek, *J. Am. Chem. Soc.* **1999**, *121*, 1601 – 1602.
[67] A. H. Romero, P. L. Silvestri, M. Parrinello, *Phys. Status Solidi B* **2000**, *220*, 703 – 708.
[68] H. S. Frank, W. Y. Wen, *Discuss. Faraday Soc.* **1957**, *24*, 133 – 140.
[69] U. C. Singh, P. A. Kollman, *J. Chem. Phys.* **1985**, *83*, 4033 – 4040.
[70] K. Morokuma, K. Kitaura, *Molecular Interactions* (Eds.: H. Ratajcak, W. J. Orville-Thomas), Wiley, New York, **1980**, pp. 21 – 87.
[71] A. E. Reed, A. E. Curtiss, F. Weinhold, *Chem. Rev.* **1988**, *88*, 899 – 926.
[72] B. F. King, F. Weinhold, *J. Chem. Phys.* **1995**, *103*, 333 – 347.
[73] F. Weinhold, *J. Mol. Struct. (THEOCHEM)* **1997**, *399*, 181 – 197.
[74] NBO 4.0 Program Manual, University of Wisconsin Theoretical Chemistry Institute Technical Report WISC-TCI-756 (USA: University of Wisconsin).
[75] R. Ludwig, unpublished results.
[76] W. K. Röntgen, *Ann. Phys.* **1892**, *45*, 91 – 97.
[77] R. O. Watts, I. J. McGee, *Liquid State Chemical Physics*, Wiley, New York, **1976**.
[78] C. A. Angell, V. Rodgers, *J. Chem. Phys.* **1984**, *80*, 6245 – 6252.
[79] G. H. Haggis, J. B. Hasted, T. J. Buchanan, *J. Chem. Phys.* **1952**, *20*, 1452 – 1465.
[80] G. Nemethy, H. A. Scheraga, *J. Chem. Phys.* **1962**, *36*, 3382 – 3400.
[81] G. E. Walrafen in *Hydrogen-Bonded Solvent Systems* (Eds.: A. K. Covington, P. Jones), Taylor and Francis, London, **1968**.
[82] H. E. Stanley, J. Teixeira, *J. Chem. Phys.* **1980**, *73*, 3404 – 3423.
[83] A. Geiger, H. E. Stanley, *Phys. Rev. Lett.* **1982**, *49*, 1749 – 1752.
[84] R. L. Blumberg, H. E. Stanley, A. Geiger, P. Mausbach, *J. Chem. Phys.* **1984**, *80*, 5230 – 5241.
[85] M. G. Sceats, R. A. Rice in *Water: A Comprehensive Treatise*, *Vol. 7* (Ed.: F. Franks), Plenum, New York, **1972**.
[86] P. A. Giguere, *J. Chem. Phys.* **1987**, *87*, 4835 – 4839.
[87] F. Sciortino, P. H. Poole, H. E. Stanley, S. Havlin, *Phys. Rev. Lett.* **1990**, *64*, 1686 – 1689.
[88] F. Scortino, A. Geiger, H. E. Stanley, *Nature* **1991**, *354*, 218 – 221.
[89] F. Scortino, A. Geiger, H. E. Stanley, *J. Chem. Phys.* **1992**, *96*, 3857 – 3865.
[90] D. J. Swanton, G. B. Bacskay, N. S. Hush, *Chem. Phys.* **1983**, *82*, 303 – 315.
[91] B. A. Zilles, W. B. Person, *J. Chem. Phys.* **1983**, *79*, 65 – 77.
[92] R. D. Amos, *Chem. Phys.* **1986**, *104*, 145 – 151.
[93] D. J. Swanton, G. B. Bacskay, N. S. Hush, *J. Chem. Phys.* **1986**, *84*, 5715 – 5727.
[94] B. J. Smith, D. J. Swanton, J. A. Pople, H. S. Schaefer III, L. Radom, *J. Chem. Phys.* **1990**, *92*, 1240 – 1247.
[95] S. C. Althorpe, D. C. Clary, *J. Chem. Phys.* **1994**, *101*, 3603 – 3609.
[96] J. K. Gregory, D. C. Clary, *Chem. Phys. Lett.* **1994**, *228*, 547 – 554.
[97] J. K. Gregory, D. C. Clary, *J. Chem. Phys.* **1995**, *102*, 7817 – 7829.
[98] J. K. Gregory, D. C. Clary, *J. Chem. Phys.* **1995**, *103*, 8924 – 8930.
[99] J. K. Gregory, D. C. Clary, *J. Chem. Phys.* **1996**, *105*, 6626 – 6633.
[100] J. K. Gregory, D. C. Clary, *J. Phys. Chem.* **1996**, *100*, 18014 – 18022.
[101] J. K. Gregory, D. C. Clary, *J. Phys. Chem. A* **1997**, *101*, 6813 – 6819.
[102] J. O. Jensen, P. N. Krishnan, L. A. Burke, *Chem. Phys. Lett.* **1995**, *246*, 13 – 19.
[103] J. O. Jensen, P. N. Krishnan, L. A. Burke, *Chem. Phys. Lett.* **1996**, *260*, 499 – 506.
[104] R. Knochenmuss, S. Leutwyler, *J. Chem. Phys.* **1992**, *96*, 5233 – 5244.
[105] D. A. Estrin, L. Paglieri, G. Corongiu, E. Clementi, *J. Phys. Chem.* **1996**, *100*, 8701 – 8711.
[106] J. Rodriguez, D. Laria, E. J. Marcea, D. A. Estrin, *J. Chem. Phys.* **1999**, *110*, 9039 – 9047.
[107] K. Kim, K. D. Jordan, T. S. Zwier, *J. Am. Chem. Soc.* **1994**, *116*, 11568 – 11569.
[108] D. J. Wales, *J. Am. Chem. Soc.* **1993**, *115*, 11180 – 11190.
[109] D. J. Wales, I. Ohmine, *J. Chem. Phys.* **1993**, *98*, 7245 – 7256; D. J. Wales, I. Ohmine, *J. Chem. Phys.* **1993**, *98*, 7257 – 7268.
[110] D. J. Wales, *Science* **1996**, *271*, 925 – 929.
[111] D. J. Wales, T. R. Walsh, *J. Chem. Phys.* **1996**, *105*, 6957 – 6971.
[112] T. R. Walsh, D. J. Wales, *J. Chem. Soc. Faraday Trans.* **1996**, *92*, 2505 – 2517.
[113] D. J. Wales, T. R. Walsh, *J. Chem. Phys.* **1997**, *106*, 7193 – 7207.
[114] D. J. Wales, M. P. Hodges, *Chem. Phys. Lett.* **1998**, *286*, 65 – 72.
[115] C. J. Tsai, K. D. Jordan, *J. Phys. Chem.* **1993**, *97*, 5208 – 5210.
[116] C. J. Tsai, K. D. Jordan, *Chem. Phys. Lett.* **1993**, *213*, 181 – 188.
[117] J. C. Li, D. K. Ross, M. I. Hayes, *J. Mol. Struct. (THEOCHEM)* **1994**, *322*, 131 – 139.
[118] L. Morrison, J.-C. Li, S. Jenkins, S. S. Xantheas, M. C. Payne, *J. Phys. Chem. B* **1997**, *32*, 6146 – 6150.
[119] M. N. Beverly, U. M. Nield, *J. Phys. Chem. B* **1997**, *32*, 6188 – 6191.
[120] L. S. Sremaniak, L. Perera, M. L. Berkowitz, *J. Chem. Phys.* **1996**, *105*, 3715 – 3721.
[121] S. S. Xantheas, T. H. Dunning, Jr., *J. Chem. Phys.* **1993**, *99*, 8774 – 8792.
[122] S. S. Xantheas, *J. Chem. Phys.* **1994**, *100*, 7523 – 7534.
[123] S. S. Xantheas, *J. Chem. Phys.* **1995**, *102*, 4505 – 4517.
[124] S. S. Xantheas, *J. Chem. Phys.* **1996**, *104*, 8821 – 8824.
[125] R. M. Badger, *J. Chem. Phys.* **1934**, *2*, 128 – 131; R. M. Badger, *J. Chem. Phys.* **1935**, *3*, 710 – 714.
[126] J. Kim, K. S. Kim, *J. Chem. Phys.* **1998**, *109*, 5886 – 5895.
[127] J. Kim, D. Majumbur, H. M. Lee, K. S. Kim, *J. Chem. Phys.* **1999**, *110*, 9128 – 9134.
[128] K. Kim, K. D. Jordan, T. S. Zwier, *J. Am. Chem. Soc.* **1994**, *116*, 11568 – 11569.
[129] F. Weinhold, *J. Chem. Phys.* **1998**, *109*, 367 – 372; F. Weinhold, *J. Chem. Phys.* **1998**, *109*, 373 – 384.
[130] R. Ludwig, F. Weinhold, *J. Chem. Phys.* **1999**, *110*, 508 – 515.
[131] A. Khan, *Chem. Phys. Lett.* **1996**, *253*, 299 – 304.
[132] A. Khan, *J. Phys. Chem. A* **1999**, *103*, 1260 – 1264.
[133] M. F. Chaplin, *Biophys. Chem.* **1999**, *83*, 211 – 221.
[134] L. J. Barbour, G. W. Orr, J. L. Atwood, *Nature* **1998**, *393*, 671 – 673.
[135] N. Pugliano, R. J. Saykally, *J. Chem. Phys.* **1992**, *96*, 1832 – 1839.
[136] N. Pugliano, R. J. Saykally, *Science* **1992**, *257*, 1937 – 1940.
[137] J. D. Cruzan, L. B. Braly, K. Liu, M. G. Brown, J. G. Loeser, R. J. Saykally, *Science* **1996**, *271*, 59 – 62.
[138] K. Liu, M. G. Brown, J. D. Cruzan, R. J. Saykally, *Science* **1996**, *271*, 62 – 64.
[139] K. Lui, J. D. Cruzan, R. J. Saykally, *Science* **1996**, *271*, 929 – 933.
[140] J. K. Gregory, D. C. Clary, K. Liu, M. G. Brown, R. J. Saykally, *Science* **1997**, *275*, 814 – 817.
[141] J. D. Cruzan, M. G. Brown, K. Liu, L. B. Braly, R. J. Saykally, *J. Chem. Phys.* **1996**, *105*, 6634 – 6644.
[142] K. Liu, M. G. Brown, R. J. Saykally, *J. Phys. Chem. A* **1997**, *101*, 8995 – 9010.
[143] M. G. Brown, F. N. Keutsch, R. J. Saykally, *J. Chem. Phys.* **1998**, *109*, 9645 – 9647.
[144] R. S. Fellers, C. Leforestier, L. B. Braly, M. G. Brown, R. J. Saykally, *Sciene* **1999**, *284*, 945 – 948.
[145] M. R. Viant, M. G. Brown, J. D. Cruzan, R. J. Saykally, *J. Chem. Phys.* **1999**, *110*, 4369 – 4381.
[146] K. Liu, M. G. Brown, C. Carter, R. J. Saykally, J. K. Gregory, D. C. Clary, *Nature* **1996**, *381*, 501 – 503.
[147] J. B. Anderson, *J. Chem. Phys.* **1986**, *63*, 1499 – 1503.
[148] D. F. Cooker, R. O. Watts, *Mol. Phys.* **1986**, *58*, 1113 – 1129.
[149] V. Buch, *J. Chem. Phys.* **1992**, *97*, 726 – 729.

[150] K. Nauta, R. E. Miller, *Science* **2000**, *287*, 293 – 295.
[151] M. Hartmann, R. E. Miller, J. P. Toennies, A. F. Vilesov, *Phys. Rev. Lett.* **1995**, *75*, 1566 – 1569.
[152] M. Behrens, R. Frochtenicht, M. Hartmann, S. Jorg-Gerald, U. Buck, *J. Chem. Phys.* **1999**, *111*, 2436 – 2443.
[153] F. Huisken, M. Kaloudis, A. Kulcke, *J. Chem. Phys.* **1996**, *104*, 17 – 25.
[154] R. Custalcean, C. Afloroaiei, M. Vlassa, M. Polverejan, *Angew. Chem.* **2000**, *112*, 3224 – 3226; *Angew. Chem. Int. Ed.* **2000**, *39*, 3094 – 3096.
[155] A. H. Narten, W. E. Thissen, L. Blum, *Science* **1982**, *217*, 1033 – 1034.
[156] L. J. Barbour, G. W. Orr, J. L. Atwood, *Chem. Commun.* **2000**, 859 – 860.
[157] U. Buck, I. Ettischer, M. Melzer, V. Buch, J. Sadlej, *Phys. Rev. Lett.* **1998**, *80*, 2578 – 2581.
[158] J. Brudermann, M. Melzer, U. Buck, J. K. Kazmirski, J. Sadlej, V. Buch, *J. Chem. Phys.* **1999**, *110*, 10649 – 10652.
[159] J. Brudermann, P. Lohbrandt, U. Buck, *Phys. Rev. Lett.* **1998**, *80*, 2821 – 2824.
[160] R. H. Page, M. F. Vernon, Y. R. Shen, Y. T. Lee, *Chem. Phys. Lett.* **1987**, *141*, 1 – 6.
[161] D. F. Coker, R. E. Miller, R. O. Watts, *J. Chem. Phys.* **1985**, *82*, 3554 – 3562.
[162] R. N. Pribble, T. S. Zwier, *Science* **1994**, *265*, 75 – 79.
[163] C. J. Gruenloh, J. R. Carney, C. A. Arrington, T. S. Zwier, S. Y. Fredericks, K. D. Jordan, *Science* **1997**, *276*, 1678 – 1691.
[164] C. J. Gruenloh, J. R. Carney, F. C. Hagemeister, C. A. Arrington, T. S. Zwier, S. Y. Fredericks, J. T. Woods, K. D. Jordan, *J. Chem. Phys.* **1998**, *109*, 6601 – 6614.
[165] U. Buck, *J. Chem. Phys.* **1994**, *98*, 5190 – 5200.
[166] R. Ludwig, T. C. Farrar, F. Weinhold, *J. Chem. Phys.* **1995**, *102*, 5118 – 5125; R. Ludwig, T. C. Farrar, F. Weinhold, *J. Chem. Phys.* **1995**, *103*, 3636 – 3642.
[167] R. Ludwig, T. C. Farrar, F. Weinhold, *J. Chem. Phys.* **1997**, *107*, 499 – 507.
[168] R. Ludwig, O. Reis, R. Winter, T. C. Farrar, F. Weinhold, *J. Phys. Chem. B* **1997**, *101*, 8861 – 8870.
[169] R. Ludwig, T. C. Farrar, F. Weinhold, *J. Phys. Chem. B* **1997**, *102*, 9312 – 9318.
[170] M. Wendt, T. C. Farrar, *Mol. Phys.* **1998**, *95*, 1077 – 1081.
[171] R. Ludwig, T. C. Farrar, F. Weinhold, *Mol. Phys.* **1999**, *97*, 465 – 477; R. Ludwig, T. C. Farrar, F. Weinhold, *Mol. Phys.* **1999**, *97*, 479 – 486.
[172] H. Huelsekopf, R. Ludwig, *J. Mol. Liq.* **2000**, *85*, 105 – 125.
[173] R. Laenen, K. Simeonidis, R. Ludwig, *J. Chem. Phys.* **1999**, *111*, 5897 – 5904.
[174] R. Ludwig, F. Weinhold, *Phys. Chem. Chem. Phys.* **2000**, *2*, 1613 – 1619.
[175] R. Ludwig, F. Weinhold, unpublished results.
[176] P. M. Wiggins, *Prog. Polym. Sci.* **1995**, *20*, 1121 – 1163.
[177] S. R. Elliot, *J. Chem. Phys.* **1995**, *103*, 2758 – 2761.
[178] O. Mishima, L. D. Calvert, E. Whalley, *Nature* **1985**, *314*, 76 – 78.
[179] A. H. Narten, M. D. Danford, H. A. Levy, *Discuss. Faraday Soc.* **1967**, *43*, 97 – 107.
[180] A. A. Chialvo, P. T. Cummings, J. M. Simonson, R. E. Mesmer, H. D. Cochran, *Ind. Eng. Chem. Res.* **1998**, *37*, 3021 – 3025.
[181] J. C. Li, P. Jenniskens, *Planet. Space Sci.* **1997**, *45*, 469 – 473.
[182] M. R. Chowdhury, J. C. Dore, D. G. Montague, *J. Phys. Chem.* **1983**, *87*, 4037 – 4039.
[183] A. Bizid, L. Bosio, L. Defrain, M. Oumezzine, *J. Chem. Phys.* **1987**, *87*, 2225 – 2230.
[184] J. C. Dore, *J. Mol. Struct. (THEOCHEM)* **1990**, *237*, 221 – 232.
[185] S. W. Benson, E. D. Siebert, *J. Am. Chem. Soc.* **1992**, *114*, 4269 – 4276.
[186] H. Bertagnolli, *Angew. Chem.* **1992**, *104*, 1615 – 1516; *Angew. Chem. Int. Ed. Engl.* **1992**, *31*, 1577 – 1578.